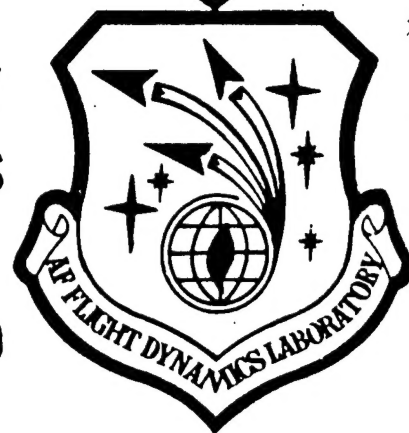AFFDL TM 78-31-FXN

AIR FORCE FLIGHT DYNAMICS LABORATORY
DIRECTOR OF LABORATORIES
AIR FORCE SYSTEMS COMMAND
WRIGHT PATTERSON AIR FORCE BASE OHIO

A STUDY TO DEVELOP OPTICAL
INSTRUMENTATION FOR THE
AFFDL RENT FACILITY

J. D. Trolinger

Spectron Development Laboratories, Inc.
Costa Mesa, California

D. M. Parobek
A. G. Stringer

Air Force Flight Dynamics Laboratory
Wright-Patterson Air Force Base, Ohio

Approved for public release; distribution unlimited.

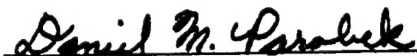February 1978

NOTICE

When Government drawings, specifications, or other data are used for any purpose other than in connection with a definitely related Government procurement operation, the United States Government thereby incurs no responsibility nor any obligation whatsoever; and the fact that the government may have formulated, furnished, or in any way supplied the said drawings, specifications, or other data is not to be regarded by implication or otherwise as in any manner licensing the holder or any other person or corporation, or conveying any rights or permission to manufacture, use, or sell any patented invention that may in any way be related thereto.
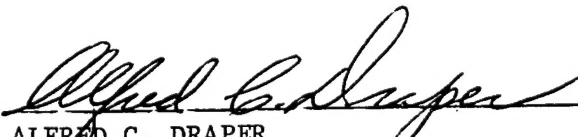
This report has been reviewed and is approved for publication.

FOREWORD

This report summarizes work carried out by both Spectron Development Laboratories of Costa Mesa, California (Dr. James D. Trolinger, Visiting Scientist) under University of Dayton Contract F33615-76-C-3145 and the Experimental Engineering Branch of the Flight Dynamics Laboratory. The developments reported were carried out under Project 1426, "Aerodynamic Ground Test Technology", Task 142601, "Diagnostic, Instrumentation and Similitude Technology", and Work Unit 14260143, "Development of Thermal and Flow Measurement Techniques." Mr. Daniel M. Parobek of the Air Force Flight Dynamics Laboratory (AFFDL/FXN) was the contract monitor as well as principal in-house engineer on the AFFDL portion of the technical work covered by this report. Mr. Arthur G. Stringer, also of AFFDL, performed experimental programs and equipment development.

The authors wish to acknowledge the effort of Mr. Henry D. Baust of the Electronics Group of the Experimental Engineering Branch for engineering assistance.

This development effort was initiated in August 1976 and was completed in September 1977.

The technical memorandum was released by the authors in October 1977 for publication.

TABLE OF CONTENTS

LIST OF ILLUSTRATIONS

LIST OF TABLES

SECTION I

INTRODUCTION

The "RENT" facility is a high-enthalpy reentry nosetip test facility which employs a 50 megawatt arc heater to produce a high energy supersonic free jet test flow. The objectives of such tests include the determination of materials' response to simulated reentry conditions, heat transfer, erosion and ablation, and other aerodynamic effects.

To attain the full utility of the facility requires both computation and measurement of the conditions and aerodynamic phenomena which occur during tests. The flow is in many respects too complex to allow accurate computation of all phenomena of interest. Therefore, measurements are needed to provide more accurate descriptions of many basic properties and phenomena.

A number of optical measurement techniques have been attempted in the "RENT" facility with some degrees of success, and programs to refine such methods have been active for several years. A study has begun recently to continue the development and application of optical diagnostic methods for this facility.

The objective of this study is to examine candidate optical measurement techniques, to plan the development of such methods, and ultimately to apply developed techniques during actual test operations.

The types of measurements under consideration include: (1) methods to observe the flowfield over the model (e.g., the bow shock, the boundary layer, turbulence, and particle/flowfield interactions), (2) eroding particle properties (e.g., particle velocity, size, and number density distribution), (3) gas velocity and turbulence, (4) temperature and density, and (5) model surface properties (e.g., profile and roughness).

1. PLANNED APPROACH

Preliminary work to some degree has already been conducted in all of the above tasks with respect to the "RENT" facility, although no operational technique has evolved. Our first task was to review all such work and to determine which methods should be pursued further. Concurrent with this task was the organizing of an internal optics laboratory capable of supporting the required optical measurements. This involved the gathering of the basic types of optics equipment needed and the establishment of an optics laboratory. A number of optical instruments were known to be available as Government Furnished Equipment (GFE) from several Air Force agencies. Contacts were made to determine the availability of such equipment and the applicability in the "RENT" facility.

The basic approach has been to assemble and test the simplest techniques first. An outline of the various problems with probable obstacles has been completed. A plan has been laid to carry the developing instruments through a series of stages of increasing complexity such that ultimately instruments will evolve which are capable of functioning in the operating "RENT" facility.

Since a considerable amount of work had been performed toward the development of a shadowgraph system and since this work was promising, the work was continued with attempts to remove the remaining obstacles to be discussed.

At the same time, plans were made to procure (as GFE) equipment with which to build a laser Doppler velocimeter ultimately to be used in the facility. The remaining areas were left to be examined as time permitted.

2. SUMMARY

As of September 1977, the status of the project is summarized below.

a. Flowfield Measurements

    (1) Previous work was reviewed and analyzed.

    (2) Laboratory tests on several concepts were performed.

    (3) A shadowgraph system of new concept was designed to meet the conditions in the "RENT" facility.

    (4) The system was mocked up and tested in the laboratory.

    (5) The chosen system was constructed and lab tested.

    (6) The system integration with the "RENT" facility was carried out.

    (7) The system is currently under test in the "RENT" facility.

    (8) Variations of the above system are being examined in the laboratory to provide improved versatility.

    (9) It has been determined that the system can also be used to perform holographic interferometry.

    (10) A number of potential applications of the system have been examined in the laboratory.

b. Eroding Particle Properties

    (1) Several system options for laser Doppler velocimeters have been identified.

    (2) Equipment options have been determined and procurement is underway.

    (3) Plans to assemble a laboratory system from GFE have been laid.

    (4) Options to use holography have also been examined.

     (5)   The required holography equipment is now in hand.

c. Gas Velocity and Turbulence

     (1)   Laser Doppler equipment will be directed toward this measurement.

     (2)   Plans for upgrading equipment in Item b. for this measurement have been made.

     (3)   Plans call for this task to evolve out of Task b.

d. Temperature and Density

    No work done to date

e. Model Surface Properties

     (1)   Surface roughness and contour techniques have been reviewed.

     (2)   Surface characteristics terminology has been reviewed and categorized for model application.

     (3)   Facility problems have been examined.

     (4)   Candidate methods have been selected.

     (5)   Plans for further experimental work have been laid.

In the following sections, a detailed description of the work performed in arriving at the above status is presented.

SECTION II
DESCRIPTION OF THE "RENT" FACILITY
FROM AN OPTICAL INSTRUMENTATION POINT OF VIEW

1. FACILITY GEOMETRY

Figures 1-3 show the "RENT" facility layout (see Reference 1). The models are injected into the arc-heated flow by a rack which holds up to five models. The models are typically conical in shape having hemispherical nosetips of diameters in the order of one inch. When injected, the tip of the model is positioned in the test rhombus and near the nozzle exit, where it heats up and ablates and/or erodes.

Instrumentation is mounted on a platform above the model. Also, shields on each side of the arc heater provide an appropriate location for instrumentation, although generally instruments cannot be located closer than about ten feet from the model.

2. ENVIRONMENTAL CONDITIONS

The environment is rather severe from an optical instrumentation standpoint. Noise and vibration conditions are harsh. Acoustical noise exceeds 100 dB. Vibration from the arc heater and nozzle exhaust rule out the use of extremely sensitive instruments, since there is currently no vibration isolation mounting frame in the facility. The construction of such a mounting would be more difficult than ordinarily is the case, since the facility is housed inside a (one-time) wind tunnel. Mounts would have to protrude through the wind tunnel wall down to the ground outside.

The electrical noise environment is also severe because of high currents and fields associated with the arc heater.

The environment is dirty by optical standards, since it is dusty and is used as a work area for mechanical and electrical
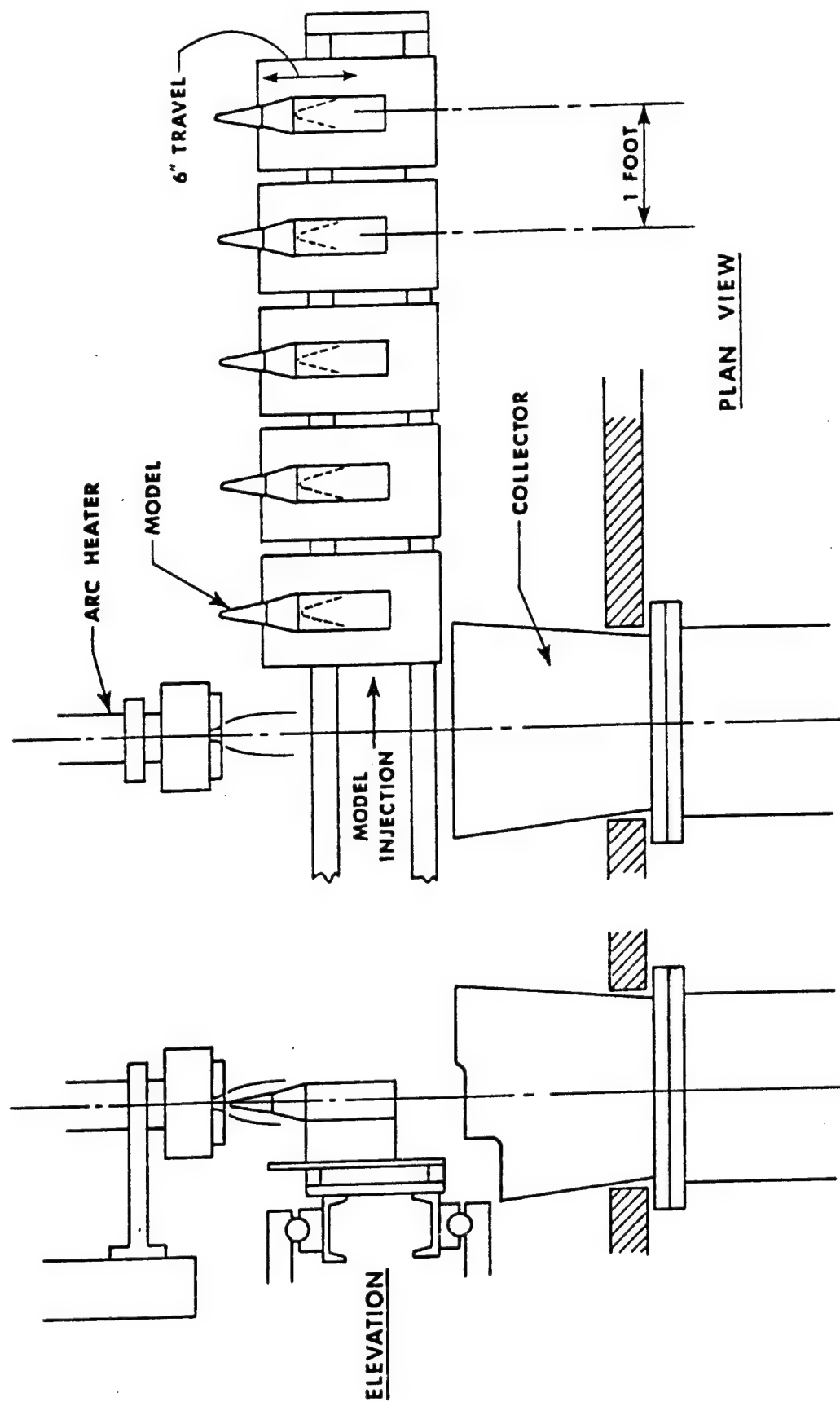
FIGURE 1. RENT TEST SECTION AND MODEL SUPPORT

SPRAY RING

MODEL ACTUATOR
SYSTEM

AXIAL DRIVE
MECHANISM

ARC HEATER

NOZZLE SECTION

FRONT SPIN COIL

AXIAL
DRIVE
SENSOR

REAR SPIN COIL
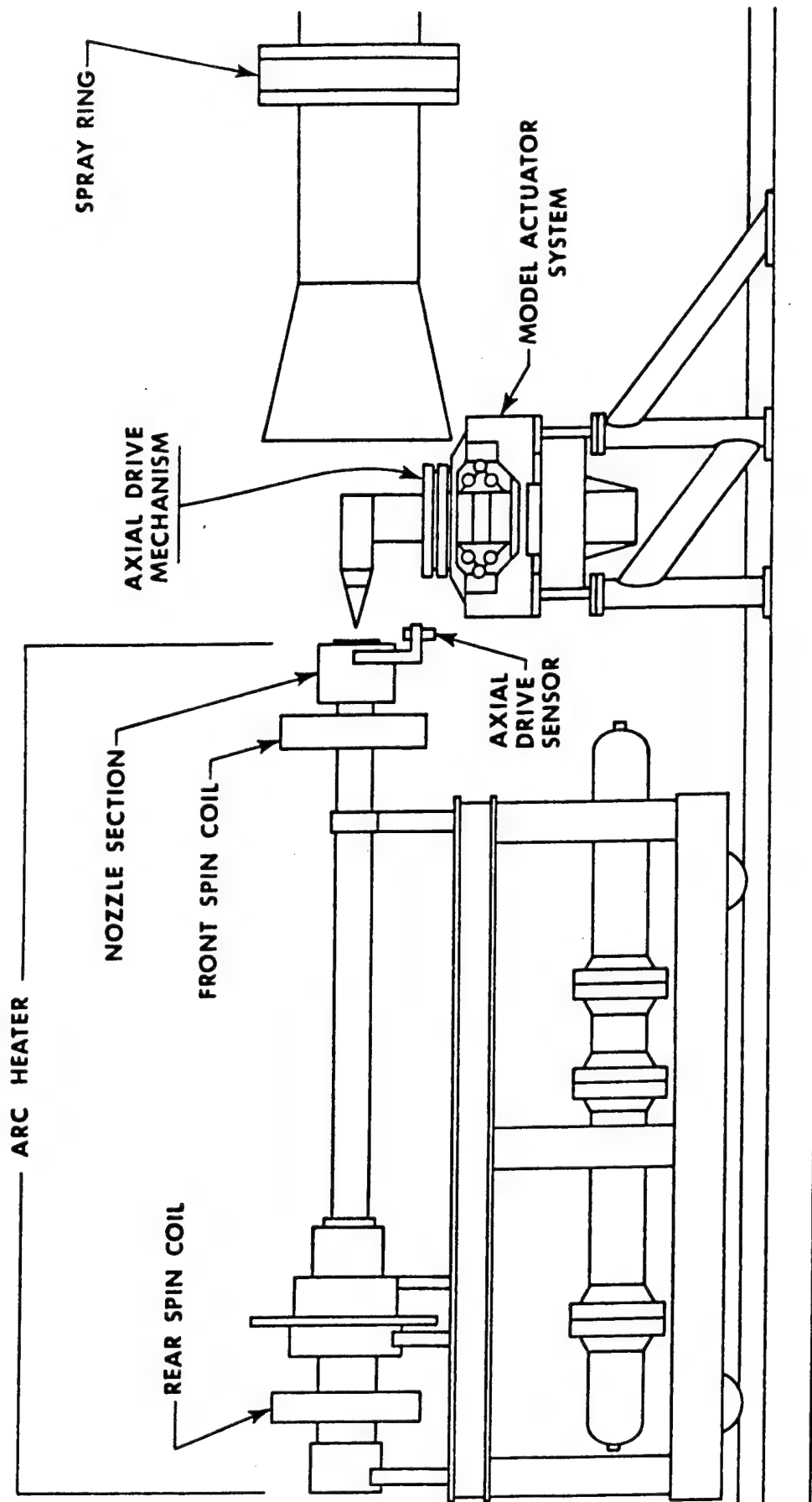
FIGURE 2. RENT TEST LEG SCHEMATIC

PENTAX CAMERA – STILL PICTURES
TOP LOCAM CAMERA – RECESSION
TOP OVERVIEW CAMERA – DOCUMENTARY

TV MONITOR

NORTH PHOTOSONICS
(PRIMARY CAMERA FOR
RECESSION & SHAPE
CHANGE)

NOZZLE EXIT
(JET COMING OUT OF PAGE)

THERMOGAGE PYROMETERS

SOUTH PHOTOSONICS CAMERA
(RECESSION & SHAPE CHANGE)

MODELS

CARRIAGE

SIDE MITCHELL CAMERA

(SHAPE CHANGE AT
ANGLE OF ATTACK
AND MONITOR)
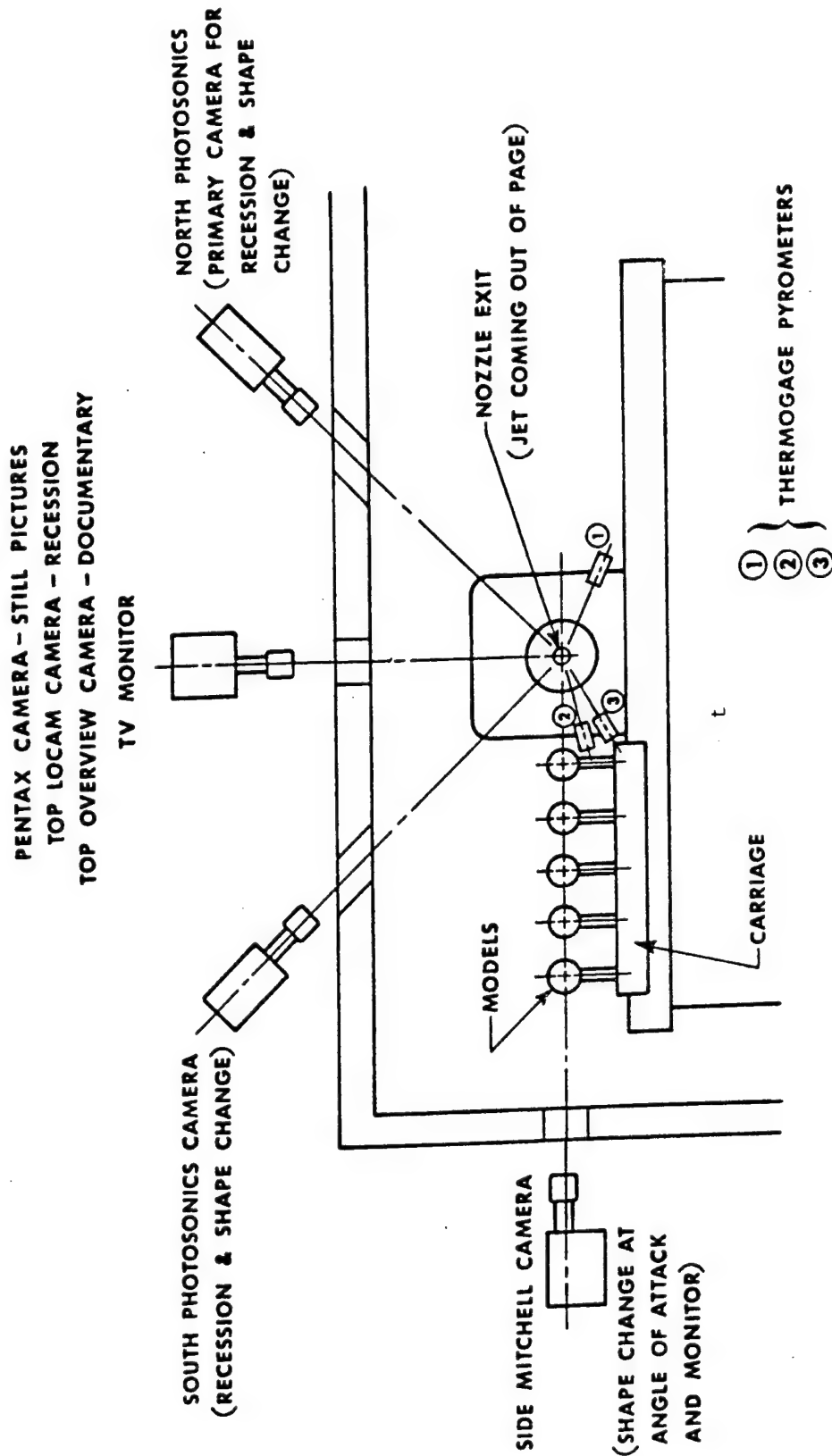
FIGURE 3.   RENT TEST SECTION PHOTOGRAPHIC COVERAGE

-8-

work, and since it is used by a fairly large number of personnel.

Ambient temperature in the lab is not well controlled and varies from about 20°C to 30°C. This creates several types of problems for optical instrumentation. Electronics associated with optical instrumentation is sometimes temperature sensitive. Critically aligned components lose alignment when temperatures vary. Temperature gradients in the air create refractive index gradients which diffract light waves causing optical noise, mis-alignment, and reduction in imaging resolution.

In particular, the model configuration is such that they are lined up in a horizontal plane. Models which have been heated and withdrawn remain in the same plane as those models under test, creating their own heat field which tends to optically obscure the model under test. Therefore, a shadowgraph system having a horizontal optical axis looks not only through the flowfield of the model under test, but also "sees" the convective flowfield about the hot, previously tested models. Previous experimental work has shown that this situation severely limits the shadow-graph and reduces the quality of the data[2]. This is a critical problem which must be solved to produce high quality shadowgraphs.

SECTION III

CANDIDATE TECHNIQUES

1. DESIRED MEASUREMENTS WHICH MAY BE ATTAINED BY OPTICAL METHODS

   a. Flow Visualization

   Optical flow visualization is one of the most widely required technologies in aerodynamic testing. Optical flow visualization is based upon the dependence of refractive index of a gas upon density. The refractive index is related to gas density approximately by the Dale-Gladstone relation

$$n = 1 + G\rho$$

where n is the refractive index, ρ is the gas density, and G is the Dale-Gladstone constant which is only weakly dependent on temperature and which varies with gas type.

   In the "RENT" facility, the density of the gas undergoes large excursions because of temperature as well as pressure effects. A flow visualization system characterizes the flow by depicting the regions of refractive index (density) changes. Therefore, shock waves, boundary layers, and turbulence are, in principle, displayed in an easily distinguishable fashion.

   The types of visualization required in the "RENT" facility are those which can provide answers to questions such as the following:

   (1) What is the spatial location and strength of shock waves?

   (2) Where and to what extent is the flow turbulent?

   (3) What is the nature of the boundary layer?

   (4) What are the conditions of flow separation?

   (5) When particles are present in the flow, what flow/particle interactions exist?

b. Surface Roughness and Contour

Model surface properties can directly influence the aerodynamics of a model. There are basically three scales of surface dimension which can be of interest. The large scale (order of millimeters) or surface contour is the dominant measure of total volume of the model and changes in the contour provides the measure of material removed by ablation and erosion.

A medium scale (hundreds of microns) provides a second order correction to material removal and also participates in aerodynamic phenomena such as flow separation and shock wave generation. It is a scale which is very important in erosion tests.

The small scale (less than 10 microns) describes the surface roughness and is thought to be most important in causing transition in the boundary layer from laminar to turbulent flow, changing the heat transfer rates to the model.

The ability to monitor surface roughness and contour is important in many types of tests. Since the tests are dynamic in character, it would be useful to monitor the various scales during the tests. Also, the surface character in most cases changes when the model is removed from the heater, so a post-test measurement is not always acceptable.

The testing of some types of models such as transpiration cooled nosetips involve the modification of the effective surface by coating it with fluid. Surface monitoring during this type of test is also of interest, although the difficulty may be even greater.

c. Particle Characteristics

When used as an erosion facility, particles are injected into the flow, after which they are further accelerated to reach a velocity as near that of the freestream as is possible. The process of injecting particles into the flow is not straightforward,

and their dispensation after injection is not completely clear. The quantities which are needed for a meaningful test are: (1) particle velocity, (2) particle size, (3) spatial distribution, and (4) number density.

None of these is easily predictable. Particle velocity lags that of the gas flow and will, in fact, be spread over a velocity distribution. Particle velocity depends upon many complex factors such as particle size, shape, mass, gas density and velocity, distance traveled, and initial velocity. Particle size depends upon agglomeration, particle break-up, initial distribution, and material. The spatial distribution likewise is a complex characteristic, depending upon properties of the flow which are not well known.

Therefore, it is important that techniques be developed to measure particle characteristics. It is possible that a facility can be calibrated, reducing the amount of measurements necessary for each test. Since this measurement is a facility property as opposed to a model property, calibration is highly desirable; but only through measurement can repeatability be determined. Expected particle conditions require an instrument capable of measuring particle sizes in the range from about 20 to 200 micron diameters traveling at velocities up to about 4000 meters/second and number densities typically one per cm^3.

d. Turbulence Diagnostics

Turbulence is believed to be an extremely important parameter in erosion/ablation facilities. Not only is the turbulence caused by the presence of the model important, but also the freestream turbulence characteristic of the facility itself is important. It has been shown that freestream turbulence can influence such things as the transition location on the model and heat transfer to the model.

To fully characterize the facility test conditions, a device is needed to monitor turbulence both in the freestream as well as in the vicinity of the model. To date, little information exists on freestream turbulence in such facilities. An instrument should be capable of measuring velocities as high as 1000 meters/second and determining turbulence intensities as high as 20 percent.

Turbulent spectral content and cell size is also of interest. Turbulent frequencies exceeding 10 KHz can be expected with cell sizes ranging from about one centimeter in the freestream to extremely small sizes in the model boundary layer.

2.   CANDIDATE METHODS AND APPROACH

   a.   Laser Shadowgraph System

Previous work (see Reference 2) provided a sufficient basis to convince us that laser shadowgraph could be adapted to the "RENT" facility to provide valuable flow visualization data. Furthermore, the data and experience gained from shadowgraph systems as a first step could provide a foundation for more advanced laser diagnostic techniques such as laser Doppler velocimetry and holographic interferometry.

Only two primary obstacles prevented previous systems from reaching a generally operational state. One was created by the extreme ambient light near the stagnation region of the model which obliterated much of the flowfield information in this region by fogging the film. The other was deterioration of the shadowgraph by previously heated models.

In examining this data, we determined that both problems could be solved by making appropriate changes in the system design.

The ambient light filtering system in the previous case consisted of a low frequency cut-off filter which removed light

-13-

below .6 microns wavelength and by using a photographic emulsion which was insensitive above .65 microns. This sum of the two was in effect a .05 micron band pass filter. An additional attempt to overpower ambient light with a 15 mwatt HeNe laser was not completely successful because of the extreme intensity near the nosetip.

These experiments suggested that the same system would have worked with a further reduction by, say, a factor of five in ambient light. This could be accomplished through use of (1) a narrower band pass filter and (2) polarization filter.

The problem of obliteration by previously heated models is more subtle. We have examined a number of possible solutions to this problem including the following:

(1)   Withdraw heated models from the field of view with the existing feed mechanism.

(2)   Force air over the heated models to remove the convection currents from the field of view.

(3)   Perform the shadowgraph from a different direction so that transillumination passes only through the field of the model under test.

The third solution is the most attractive since it does not alter current test procedures. Therefore, we explored the possibility of performing shadowgraph along optical axes other than horizontal.

The problem now faced with such a geometry is providing an optical element beneath the model rack to either collect and record or to return the light back to a recording system. The space beneath the model rack is highly restrictive on such components. Placing a return mirror beneath the model is undesirable because it constitutes a double pass system and also because it is exposed to severe contamination.

This led us to the choice of using indirect shadowgraph methods. Figure 4 illustrates the concept. Light passes through the flowfield forming the shadowgraph on a back-drop plate. A photograph of this place is called an indirect shadowgraph and it can be produced from any location where optical access to the plate is available.

The geometry of the facility restricts the location of the recording camera essentially to the same line of sight as the illuminating beam. Therefore, we chose to build a telecentric system wherein the optical axis of the illuminator and receiver are the same. This allowed us to use retroreflective material as the backstop to improve the optical collection efficiency of the system. Such material is inexpensive and can be replaced frequently as it becomes contaminated.

Figure 5 shows the system design. The laser source, A, is expanded, B, onto a turning mirror, C, which directs the diverging light along the receiver optical axis. The light expands over the model onto the retroreflective surface, D, which is positioned beneath the model. The receiving system is focused on the retroreflective surface. The mirror, C, blocks the central portion of the return light, but since the surface, D, acts as a highly efficient directional diffuser, its entire image (except for the shadow of the model) is passed through the lens, E, where it is focused at the electronic shutter, F. An 0.1 micron narrow band filter, G, is placed immediately behind the shutter to remove ambient light. A second lens system, H, images the shutter plane onto the 35 mm film plane, I.

The design equations for the optical system are presented in Appendix I.

The ruby laser is charged remotely from the control room just prior to model injection. The film is advanced to a new frame by the motor drive. The fire switch operates the focal plane shutter of the camera which trips the flash contact within
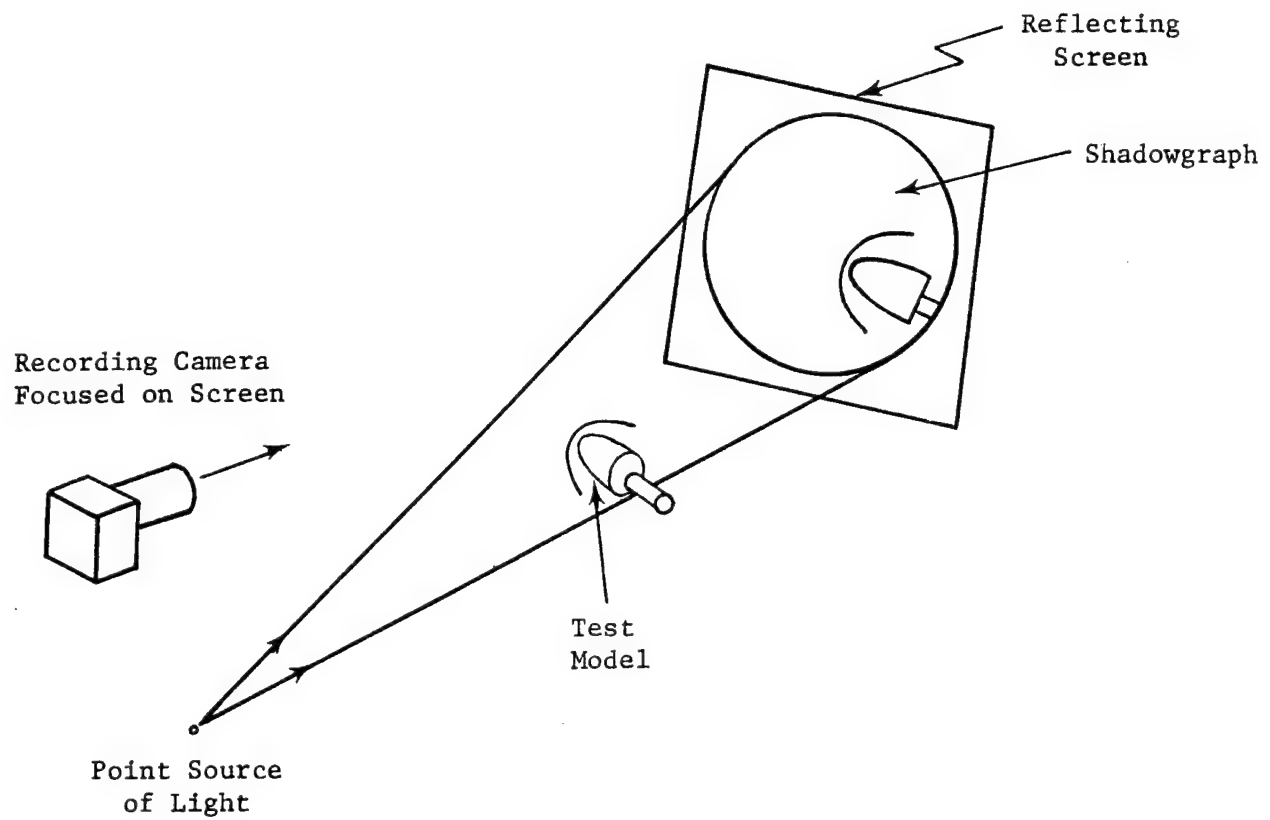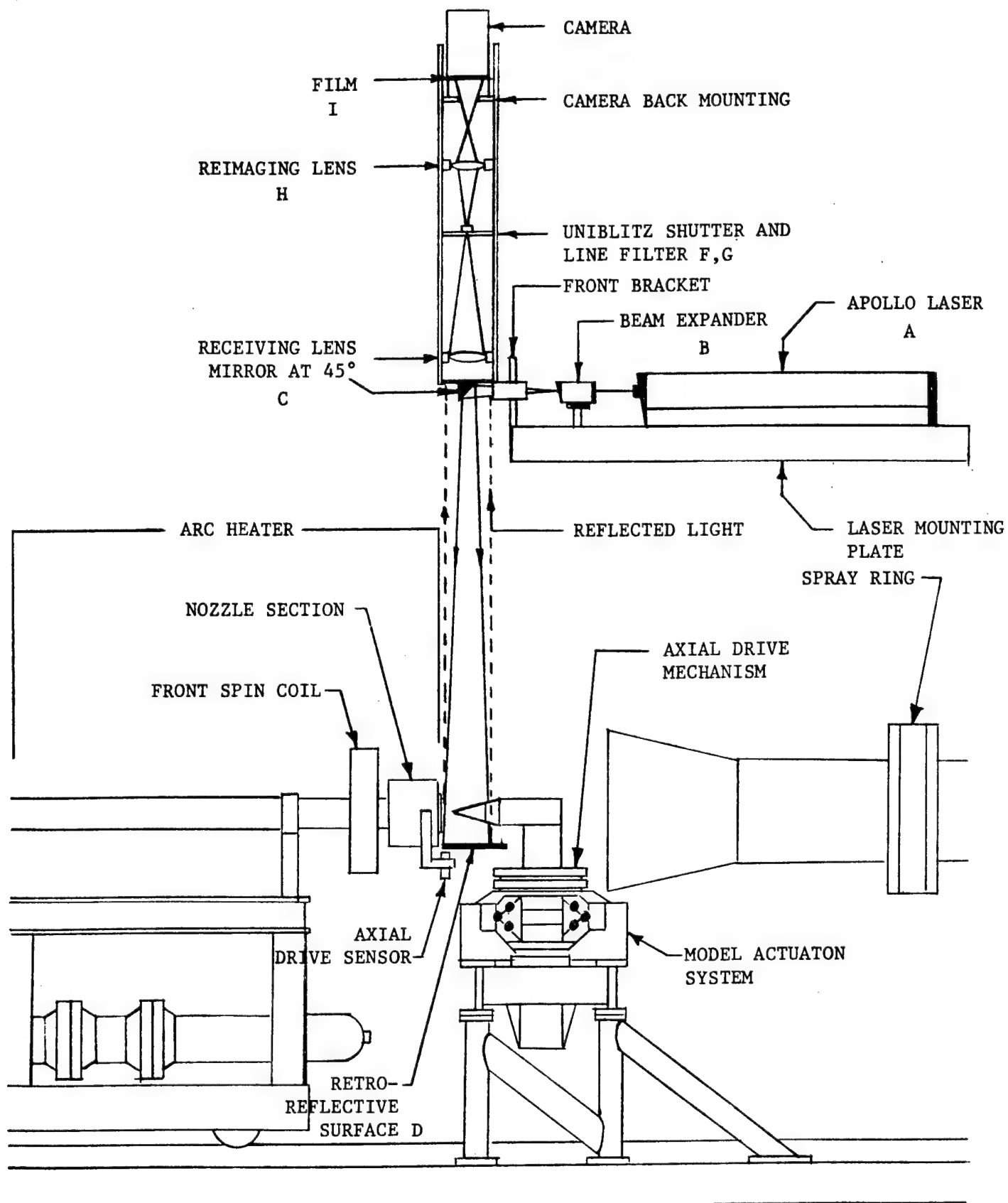
Figure 4.   Concept of Indirect Shadowgraph

Figure 5. Overhead Indirect Shadowgraph System

the camera which in turns opens the electronic shutter. Contacts on the electronic shutter then fire the ruby laser when it reaches full open position. The electronic shutter remains open for one millisecond during which time ambient light in the range .6930 to .6960 microns can pass the narrow band filter.

The control circuitry and wiring diagrams for this system are included in Appendix II.

The film transport is a Nikon motorized camera body. Film types planned for use include Kodak Tri-x and 2475 recording films, both having extended red response. The camera back was designed to also accept a larger film transport such as the Beattie-Coleman type as well as the Milliken high speed camera.

Figure 6 shows the system as built with protective shield removed.

The system has been designed to accept two existing lasers, a Spectra-Physics Model 124 15 mw HeNe continuous wave laser, and an Apollo pulsed ruby oscillator/amplifier laser. The Apollo laser is equipped with a double pulsing Pockel's cell Q-switch which provides the capability to produce two Q-switched pulses spaced in time by an amount which is adjustable from one microsecond to approximately 500 microseconds. This system will provide a method to study dynamic events by shadowgraph.

The continuous laser will be incorporated into the system in conjunction with a high-speed movie camera to provide examination of events over a long time period. It is anticipated that the two laser systems will provide a complimentary capability. The ruby laser, on the one hand, provides an extremely fine time resolution (20 nanoseconds pulse duration) with adjustable pulse separation allowing the resolution of extremely fine turbulence scales, while the HeNe system time averages each exposure over longer time, depending upon the camera speed.
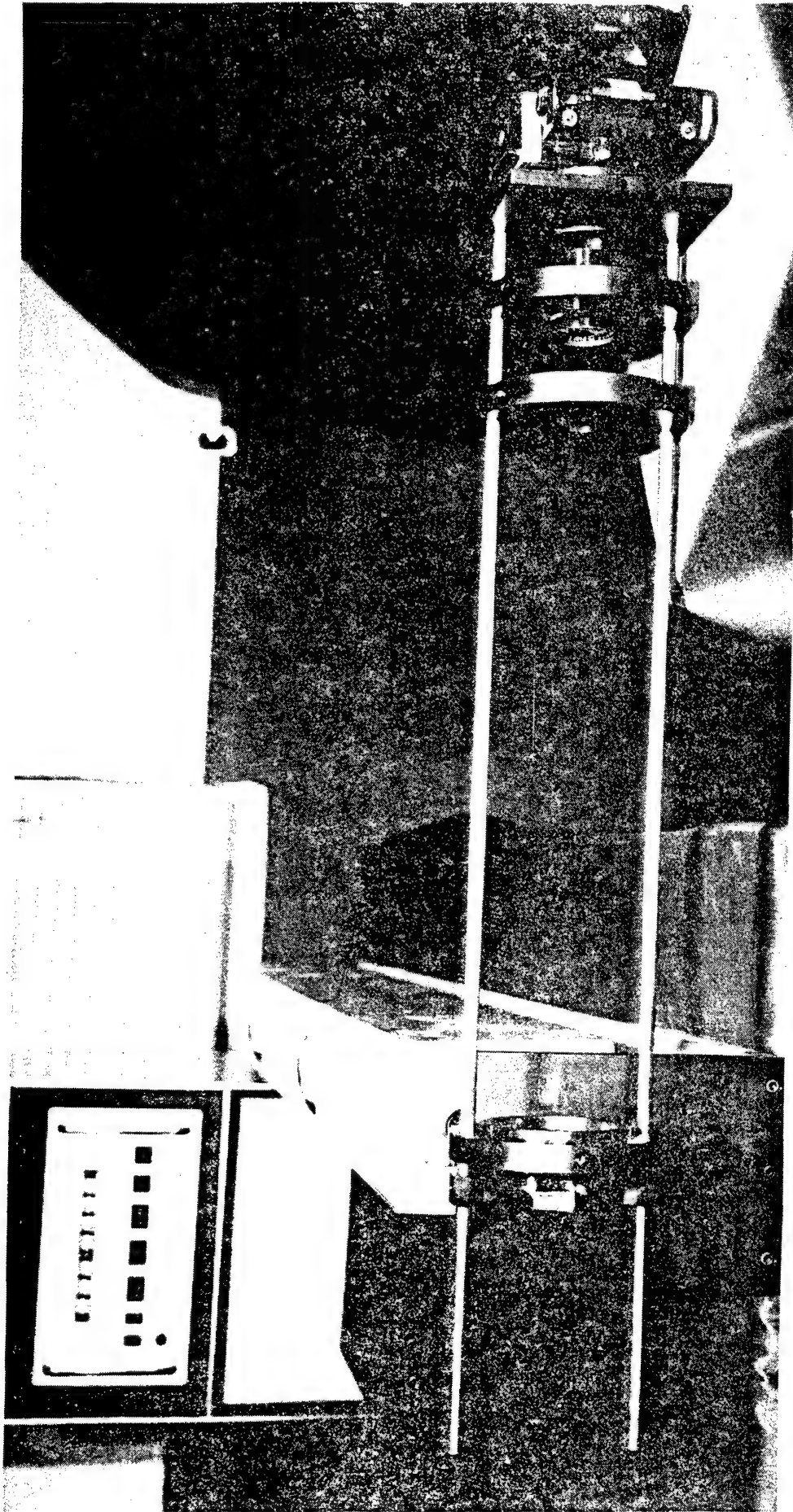
Figure 6. Laser Shadowgraph System -- (a) Side View
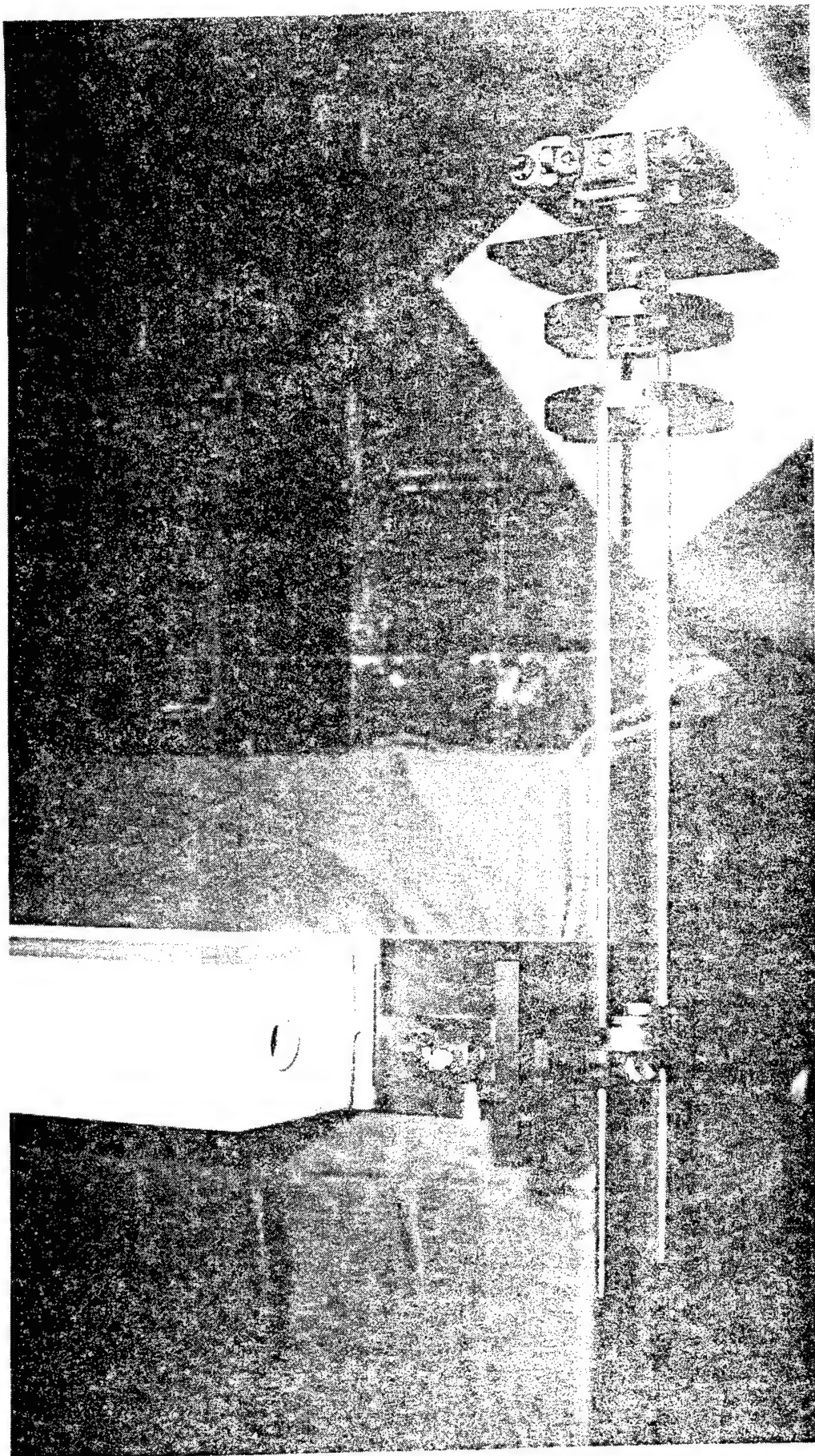
Figure 6 (Cont'd). Laser Shadowgraph System -- (b) Top View

Table 1 includes a table showing exposure time for the movie camera as a function of camera frames per second.

Time averaging to smooth out effects of turbulence is a standard practice in aerial photographs. The requirement is that the averaging time be large compared to the turbulence cell occupancy time in the image. A similar smoothing of the image can be achieved with the ruby laser system through either multiple pulsing or through operation of the laser in its normal (not Q-switched) mode. The normal mode pulse time for the existing laser lasts up to about two milliseconds.

b. Holographic Flow Visualization

Depending upon the results of the shadowgraph data, it may be desirable to exercise the option of using holography for flow visualization. The shadowgraph system has been designed so that if this option is chosen, its conversion to a holography system will be straightforward. A reference beam can be split from the laser output at a point near the beam expander and turned parallel to the receiving system optics. This beam will then be folded back into the optical train near the recording back where it is mixed with the information wave forming a hologram.

The film type for recording holograms is either Agfa-Scientia 8E75 or 10E75 roll film which comes in either 35mm or 70mm format.

This configuration was bench tested and shown to provide excellent holographic interferograms of flowfields. Figure 7 shows typical recordings of a convective heat field generated by heated metal wires.

The possible advantages of using holography as opposed to shadowgraph include: (1) holography will be less sensitive to ambient light, and (2) the flowfield can be observed while focusing on the model. The principal disadvantage is that the

Table I. Exposure Versus Frame Rate for Milliken High Speed Camera

FRAME RATE, F. P. S.

SHUTTER OPENINGS	4	8	12	16	24	32	48	64	100	128	200	250	400	500
160°	$\frac{1}{9}$	$\frac{1}{18}$	$\frac{1}{25}$	$\frac{1}{35}$	$\frac{1}{50}$	$\frac{1}{70}$	$\frac{1}{100}$	$\frac{1}{140}$	$\frac{1}{225}$	$\frac{1}{300}$	$\frac{1}{450}$	$\frac{1}{550}$	$\frac{1}{900}$	$\frac{1}{1100}$
140°	$\frac{1}{10}$	$\frac{1}{20}$	$\frac{1}{30}$	$\frac{1}{40}$	$\frac{1}{60}$	$\frac{1}{80}$	$\frac{1}{120}$	$\frac{1}{160}$	$\frac{1}{250}$	$\frac{1}{350}$	$\frac{1}{500}$	$\frac{1}{650}$	$\frac{1}{1000}$	$\frac{1}{1300}$
120°	$\frac{1}{12}$	$\frac{1}{24}$	$\frac{1}{35}$	$\frac{1}{50}$	$\frac{1}{70}$	$\frac{1}{100}$	$\frac{1}{140}$	$\frac{1}{190}$	$\frac{1}{300}$	$\frac{1}{375}$	$\frac{1}{600}$	$\frac{1}{750}$	$\frac{1}{1200}$	$\frac{1}{1500}$
72°	$\frac{1}{20}$	$\frac{1}{40}$	$\frac{1}{60}$	$\frac{1}{80}$	$\frac{1}{120}$	$\frac{1}{180}$	$\frac{1}{250}$	$\frac{1}{325}$	$\frac{1}{500}$	$\frac{1}{650}$	$\frac{1}{1000}$	$\frac{1}{1250}$	$\frac{1}{2000}$	$\frac{1}{2500}$
60°	$\frac{1}{24}$	$\frac{1}{50}$	$\frac{1}{70}$	$\frac{1}{100}$	$\frac{1}{140}$	$\frac{1}{190}$	$\frac{1}{300}$	$\frac{1}{375}$	$\frac{1}{600}$	$\frac{1}{750}$	$\frac{1}{1200}$	$\frac{1}{1500}$	$\frac{1}{2400}$	$\frac{1}{3000}$
36°	$\frac{1}{40}$	$\frac{1}{80}$	$\frac{1}{120}$	$\frac{1}{160}$	$\frac{1}{250}$	$\frac{1}{325}$	$\frac{1}{475}$	$\frac{1}{650}$	$\frac{1}{1000}$	$\frac{1}{1300}$	$\frac{1}{2000}$	$\frac{1}{2500}$	$\frac{1}{4000}$	$\frac{1}{5000}$
18°	$\frac{1}{80}$	$\frac{1}{160}$	$\frac{1}{250}$	$\frac{1}{325}$	$\frac{1}{475}$	$\frac{1}{650}$	$\frac{1}{950}$	$\frac{1}{1300}$	$\frac{1}{2000}$	$\frac{1}{2500}$	$\frac{1}{4000}$	$\frac{1}{5000}$	$\frac{1}{8000}$	$\frac{1}{10000}$
10°	$\frac{1}{140}$	$\frac{1}{300}$	$\frac{1}{425}$	$\frac{1}{600}$	$\frac{1}{850}$	$\frac{1}{1200}$	$\frac{1}{1700}$	$\frac{1}{2300}$	$\frac{1}{3500}$	$\frac{1}{4500}$	$\frac{1}{7000}$	$\frac{1}{9000}$	$\frac{1}{14000}$	$\frac{1}{18000}$
$7\frac{1}{2}°$	$\frac{1}{190}$	$\frac{1}{400}$	$\frac{1}{600}$	$\frac{1}{750}$	$\frac{1}{1200}$	$\frac{1}{1500}$	$\frac{1}{2300}$	$\frac{1}{3000}$	$\frac{1}{4800}$	$\frac{1}{6000}$	$\frac{1}{9500}$	$\frac{1}{12000}$	$\frac{1}{19000}$	$\frac{1}{24000}$

-22-

Figure 7. Holographic Subtraction Interferograms

recording is a hologram and the flowfield image must be reconstructed by laser light.

c. Surface Roughness and Contouring

As a prerequesite to choosing candidate methods for surface roughness monitoring, we examined the defining terms for surface characteristics descriptions. We then investigated existing techniques for measuring the defined characteristics. Some of the characteristics are actually defined in terms of measured parameters which must be used in conjunction with theoretical analyses to relate them to physical surface properties.

The following is a listing of techniques and definitions under consideration.

(1) Types of Measurement Techniques

(a) Tactile testing
(b) Hydraulic method
(c) Pneumatic method
(d) Capacitance method
(e) X-ray method
(f) Electron microscope
(g) Simple microscope
(h) Comparison microscope
(i) Interference method
(j) Profilometer
(k) Gloss measurement
(l) Specular reflection measurement
(m) Bi-directional reflectance measurement
(n) Speckle pattern and diffraction pattern methods

The only candidates are non-contact and fast measuring instruments (i.e., (g), (h), (i), (k), (l), (m), (n). Appendix C includes a discussion of non-imaging optical methods for surface roughness.

-24-

The critical unknown is the effect of the turbulent flow and boundary layer on these measurements.

    (2)   Surface Roughness Definitions (Figure 8, 9)

        (a)   Real Surface - The surface limiting the body, separating it from surrounding space.

        (b)   Real Profile - The contour that results from the intersection of the real surface by a plane conventionally defined with respect to the geometrical surface.

        (c)   Geometrical surface (nominal surface) - The surface determined by the design, neglecting errors of form and surface roughness.

        (d)   Geometrical profile (nominal profile) - The profile that results from the intersection of the geometrical surface by a plane conventionally defined with respect to this surface.

        (e)   Effective surface (measured surface) - The close representation of a real surface obtained by instrumental means.

        (f)   Effective profile (measured profile) - The contour that results from the intersection of the effective surface by a plane conventionally defined with respect to the geometrical surface.

        (g)   Irregularities - The peaks and valleys of a real surface.

        (h)   Spacing - The average distance between the dominant peaks on the effective profile.

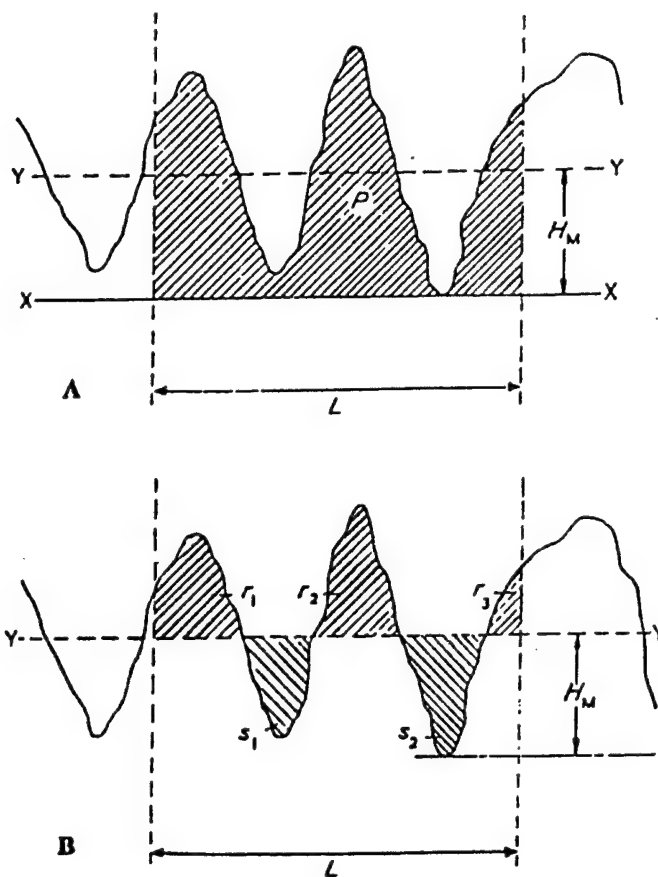   (i)   Surface Texture - Those irregularities with regular or irregular spacing which tend to

Figure 8.   Graphical Determination of R_a Values
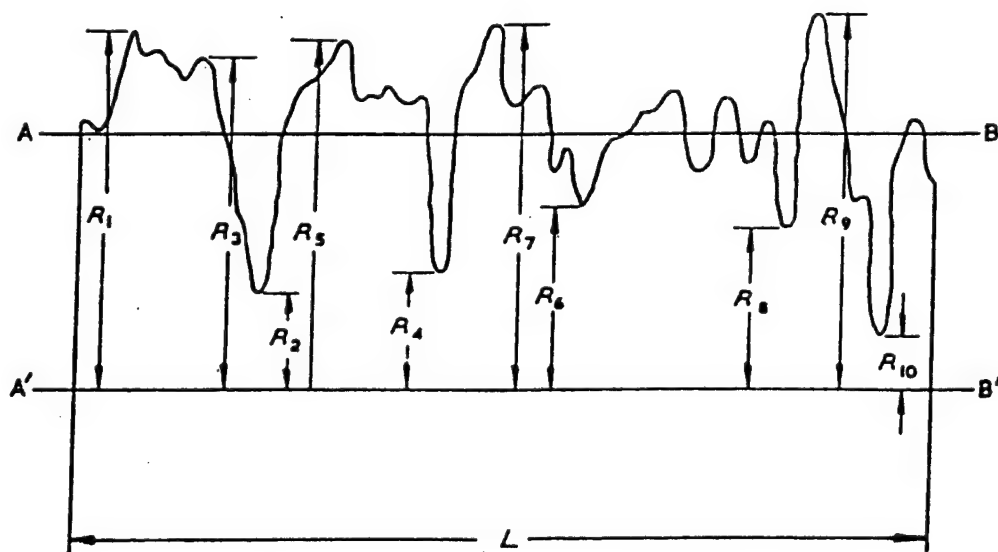
Figure 9.   Graphical Determination of R_z Values

form a pattern or texture on the sur-
face.   This texture may contain the
following components:

(1)   Roughness.   The irregularities in
      the surface texture which are in-
      herent in the production process
      but excluding waviness and errors
      of form.

(2)   Waviness - That component of sur-
      face texture upon which roughness
      is superimposed.   Waviness may
      result from such factors as mac-
      hine or work deflections, vibra-
      tions, chatter, heat treatment or
      warping strains.

(j)   Lay - The direction of the predominant
      surface pattern, ordinarily determined
      by the production method used.

(k)   Sampling Length - The length of profile
      selected for the purpose of making an
      individual measurement of surface texture.

(1)   Reference Line - The line chosen by con-
      vention to serve for the quantitative eva-
      luation of the roughness of the effective
      profile.

(m)   Center Line - A line representing the form
      of the geometrical profile and parallel to
      the general direction of the profile through-
      out the sampling length, such that the sums
      of the areas contained between it and those
      parts of the profile which lie on each side
      of it are equal.

(n)   Least-Squares Mean Line - A reference line
      representing the form of the geometrical

profile within the limits of the sampling length, and so placed that within the sampling length the sum of the squares of the deviations of the profile from the mean line is a minimum.

(o) Meter Cut-off (B_{max}) - In a profile meter instrument, the conventionally defined wavelength separating the transmitted from the attenuated components of the effective profile.

(p) Electrical Mean Line - In an electric meter instrument, a reference line established by the circuits determining the meter cut-off, which line divides equally those parts of the modified profile lying above and below it.

(q) Modified Profile - The effective profile modified by such defined filter means as are used for suppressing those undulations of the real profile that are not or are not fully to be included in the measured roughness parameters of the surface.

(r) Arithmetical Mean Deviation (R_a) - The arithmetical average value of the departure of the profile above and below the reference line (center or electrical mean line) throughout the prescribed sampling length (See Figure 9).

(s) Ten Point Height (R_z) of Irregularities - The average distance between the five highest peaks and the five deepest valleys within the sampling length, measured from a line parallel to the reference line and not crossing the profile (See Figure 10).

Waviness

Lay
(direction of
dominant pattern)

Roughness

Roughness
spacing

Profile

Waviness
spacing

90°

α
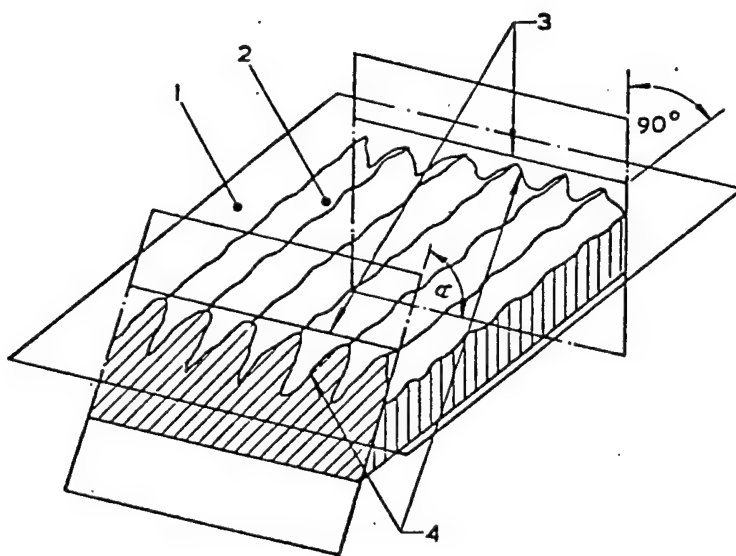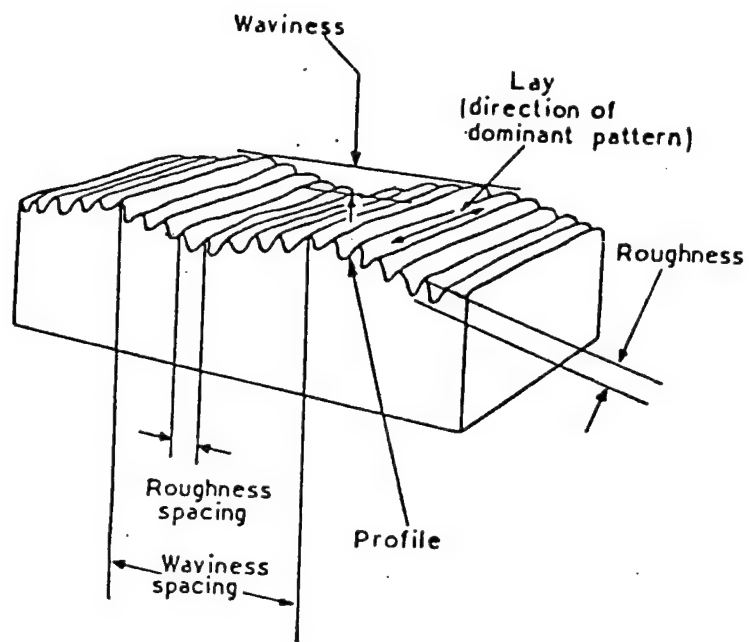
1. Geometrical surface
2. Effective surface
3. Geometrical profile
4. Effective profile

1

2

3

4

Figure 10. Surface Characteristics and Terminology

(t) Profile Recording Instrument - An instrument recording the coordinates of the profile of the surface.

(u) Recording Traversing Length - The maximum recording movement of the stylus along the surface.

(v) Profile Meter Instrument - An instrument used for the measurement of surface texture parameters.

(w) Measuring Traversing Length - The length of the modified profile used for measurement of surface roughness parameters (It is usual for the measuring traversing length to contain several sampling lengths.).

(x) Profile Meter Instrument with Predetermined Measuring Traversing Length - An instrument in which the length used for measurement has a defined beginning and end determined by switches or other instrumental means.

(y) Profile Meter Instrument with "Running" Measuring Traversing Length (giving a running average) - An instrument in which the length used for measurement results from the characteristics of the profile meter and moves along the surface with the pickup.

(3) Current Methods in Model Testing

At the present time examination of model surfaces during testing is extremely limited. Such measurements are limited to measurement of recession rates and features of the order of 100 microns or larger. This is achieved almost exclusively by

macro photography or stereo macro photography. Even these techniques are in preliminary stages of development. A laser stereo photography system has been tested, for example, on the AEDC K-track producing good quality stereo photography pairs with resolution to about 25 microns. Macro photography and stereo holography has been used with some degree of success in the RENT facility. Observed resolutions have been limited to about 100 microns in lateral dimension and several hundreds of microns in depth dimensions.

Although the model is stationary in the RENT facility, the extreme temperatures (causing high levels of ambient light) and turbulence (reducing optical resolution) make the achievement of higher resolution difficult. Furthermore, ablating models are shrouded by a boundary layer which can be laded with ablated material. Therefore, in the worst cases, the boundary layer itself could become opaque, making optical viewing of the surface impossible. The ultimate limit of such a system has yet to be determined in the RENT facility.

In the development of imaging techniques two schools of thought can be distinguished regarding the illumination methods. Since the model is self-luminous, it might seem reasonable simply to photograph the surface through an ordinary camera at high magnification using stereo photography to provide depth measurements. This could represent a very simple solution.

The high resolution photography of a self-luminous object at uniform temperature is not, however, a straightforward task. Resolution in photography depends directly on the object contrast. Contrast between various points on a self-luminous object are extremely poor in the absence of temperature gradients since no shadows exist as normally is the case when the object is illuminated externally. Therefore, in the design of such a system, all optics and film must be chosen to compensate for this loss of contrast. During an actual test, the aerodynamics and

and heat transfer should relax this problem by creating temperature gradients which are actually associated with the surface roughness. This effect should improve the ability to view roughness elements by this method and conceivably provide a qualitative observation of heat transfer variations. Prototype Development Associates (PDA) has considered measurements of this type in the RENT Facility.

The alternate approach has been to illuminate the model externally. External illumination would provide higher contrast and, in principle, higher attainable resolution, but the problem of model luminosity must then be solved. Such a system was developed by Science Applications, Inc. (SAI) and tested in the RENT Facility in 1975. The system employed a pulsed YAG laser operating at .53 microns wavelength. Ambient light was removed by (1) narrow band filters, (2) polarization filters, and (3) a fast Kerr cell shutter which remained open for less than 10^{-7} seconds. The laser pulse duration was about $2x10^{-8}$ seconds. Photographs and holograms of the surface of an oblating model were successfully produced; however, coherent speckle limited the imaging resolution to approximately 100 microns. The final report describing the details of this application has not been published at this time.

The bulk of fine surface detail measurements currently are post test measurements. The model or a replica is scanned by a stylus profilometer to provide numbers as small as the stylus diameter, typically down to about five microns. In addition to this method, the model or its replica is often sectioned and studied with microphotography to provide specific numbers. Optical comparators are used to examine profiles, but cannot display concave parts of the models (e.g., craters).

In most cases a model undergoes mechanical and thermal shocks after testing that cause changes in the surface condition. Therefore, post test surface diagnostics cannot be expected

to be reliable or accurately representative of the surface during testing. Also, post test analysis does not allow the direct observation of surface/aerodynamic interaction. Clearly, in-situ surface diagnostics are needed. Also, it is clear that the methods used for post-test analysis cannot be used for in-situ analysis. It is important that the method chosen for in-situ analysis provides measures that can be easily related to post-test measurements and to quantities which are of significance in the material response.

Surface roughness is of particular importance because of its effect on the boundary layer. Peaks in the surface trip the boundary layer and cause transition, thus affecting heat transfer to the model. The height and spacing of such peaks can be used in models for the flow to determine heat transfer. Therefore, if an instrument can provide RMS peak height and spacing, it is probably satisfactory as a roughness measurement tool. The precise measure of surface profile is likely to provide more data than is actually needed in present models, since the models themselves are statistical.

Imaging techniques are satisfying to use because the surface itself is actually viewed by the observer. Therefore, the development of imaging techniques should be continued. However, a scattering instrument has the potential of performing the required measurement in a more easily useable form. Therefore, we have examined scattering properties of some materials of interest. It appears feasible to relate scattering properties of specific materials to measurements made in a typical post-test analysis through calibration of sample surfaces; however, additional study will be required to insure that this is the case.

d. Laser Doppler Velocimetry

(1) Basic Description

Laser Doppler instruments can be used for particle velocity measurement as well as size measurement. The principle

of operation can be explained in terms of Doppler shift of light
by a moving scatterer (frequency shift proportional to velocity)
or more simply, in terms of interferometry. (See Reference 3.)
When two beams of coherent light are mixed in space, they inter-
fere, causing alternate light and dark sheets, or interference
fringe planes (See Figure 11). The fringe planes are separated
by a distance which is easily calculated. A typical fringe plane
separation is about ten microns, depending upon the desired mea-
surement range.

Velocity is measured by detecting the scattered
light and measuring the time required for a particle to travel
from one bright fringe to the next. This provides the velocity
component normal to the fringe planes. This measurement is pro-
vided by a counting processor which is termed a Doppler burst
counting processor. A Doppler burst is the signal generated by
a single scatter center traversing the fringes in the sample vol-
ume, usually about 15 fringes. The processor must incorporate
noise rejection circuitry to insure that only valid Doppler sig-
nals are analyzed. (See Reference 3).

Particle size is also determined by the Doppler
signal characteristics. The scattered signal is superimposed upon
a Gaussian shaped pedestal (See Figure 11), the level of which in-
creases as the particle diameter approaches the fringe spacing.
The signal excursions range from their highest value when the par-
ticle is centered on a bright fringe to their lowest value when
centered on a dark fringe. The difference between the high and
low values defines a quantity known as signal contrast. The con-
trast is largest for small particles and becomes decreasingly
small with increasing particle size. The measurable range is from
about 0.1 fringe spacing up to one fringe spacing.

(2) The Approach

The possible applications of the laser Doppler ve-
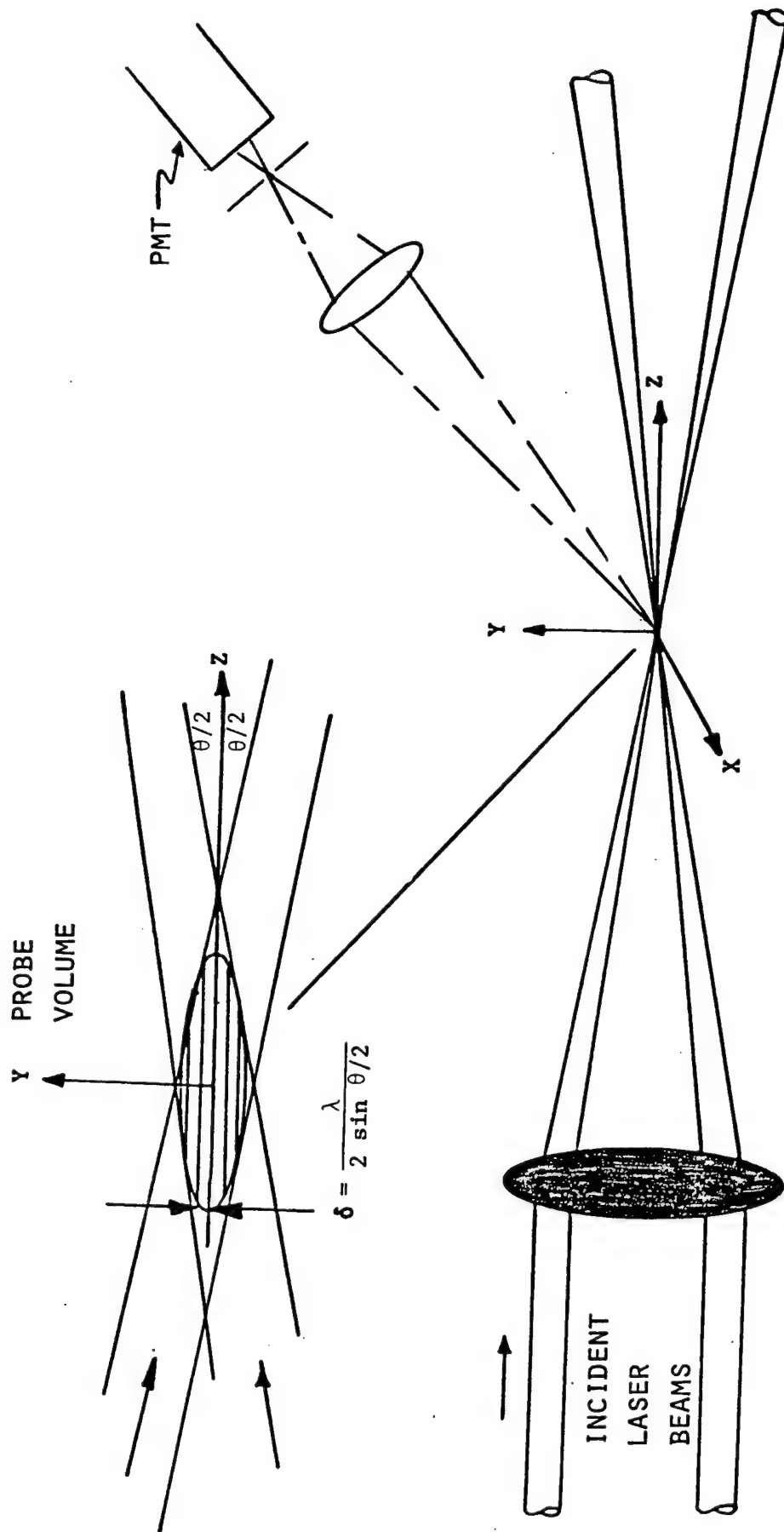locimeter include (1) erosive particle velocity, (2) erosive

Figure 11. Fringe Formation in the Sample Volume

$$\delta = \frac{\lambda}{2 \sin \theta/2}$$

PROBE
VOLUME

PMT

INCIDENT
LASER
BEAMS

-35-

particle size, (3) gas velocity and turbulence around the model. The measurements are required both outside the facility for calibration of facility components (i.e., the particle injector), and in the facility for diagnostics during testing.

The range of difficulty increases from items one to three as well as in the application during testing. The following factors must be considered in choosing the most logical approach:

(a) Erosive particles are relatively large (~30-80 microns) and are excellent scattering centers.

(b) The velocity of erosive particles ranges up to 4000 m/sec while gas velocity in the model environment ranges up to 1000 m/sec.

(c) An optical system for laboratory application is much simpler than that for the RENT Facility.

(d) Particles smaller than one micron will track the gas velocity of interest.

(e) The Mie scattering cross section is proportional to particle diameter squared so we can expect 10^4 to 10^6 more scattered light for erosive particles than for those tracked to determine gas velocity.

Laser Doppler instruments for this type of application represent the very state of the art, and "turn key" systems do not exist. The availability of two GFE systems, however, suggested a logical approach to meeting these requirements.

An existing system which is part of a diagnostic equipment inventory of the Space and Missile Systems Organization

(SAMSO) is currently being prepared for use at the Arnold Engineer-
ing Development Center (AEDC) in a similar application. It will
be available for use at WPAFB in the fall of 1977.

In the meantime, a similar component type of system
at AEDC was immediately available for use at WPAFB. Therefore,
the approach was to begin as soon as possible with the use of the
available laser Doppler system in laboratory calibrations so that
an in-house capability will exist and so that FDL personnel can
become familiar with its use and the handling of LDV data.

The available system was moved to WPAFB from the
AEDC Range G Facility. Eugene D. Tidwell was the principal con-
tact at AEDC. Assembly of the LDV system began in January 1977.

SECTION IV

CONCLUSIONS AND RECOMMENDATIONS

The laser shadowgraph system is currently installed in the
RENT Facility. Checkout of this system should be completed in
October 1977. We expect to learn a considerable amount from the
data derived from this system and will base future work for re-
finement and advanced development on these results.

The Laser Doppler System was set up and checked out in the
laboratory. This system became operational in July. Preliminary
work involved the system testing by simulated high speed particle
injection. The methods of system alignment and data acquisition
were examined during these tests. The system was also checked
for accuracy.

In August this system was used in a feasibility test in the
two foot trisonic wind tunnel. The results of these tests will
be presented in a separate report.

Surface roughness measurement candidates for laboratory
checkout were described. The laser shadowgraph system can also
serve as a macro-photography station for surface analysis. The
potential for this purpose can be considered during the future
test phase of the shadowgraph system. The conversion of this
method to produce stereo surface photography would also be straight-
forward.

Based upon these studies, we concluded that:

(1) A laser shadowgraph station could be successfuly
     operated in the RENT Facility Environment;

(2) The ruby laser system could provide extremely
     high time resolution and could through multiple
     pulsing provide a certain degree of averaging
     as well as some display of dynamic phenomena.

(3) A helium neon laser system could also be employed
    to provide longer time averaged shadowgraph to
    smooth out turbulence effects.

(4) Laser Doppler instruments can be used to provide
    diagnostics for erosive particle velocities and
    size and for the diagnostics of free stream tur-
    bulence.

(5) The diagnostics of free stream turbulence will
    be the most difficult task.

(6) The existing laser Doppler system was tractable
    to the FDL Trisonic tunnel under the proper seed-
    ing conditions.

(7) A variety of surface roughness measurement tech-
    niques now exist as candidate devices. The
    most likely candidates for the RENT facility
    include stereo photography and light scatter-
    ing methods.

We recommend that:

(1) The laser shadowgraph system be continually refined
    and that knowledge provided from the resulting data
    be available for other instrument developments.

(2) The FDL in-house laser Doppler system be expanded
    and completed for general use in the laboratories,
    wind tunnels, and in the RENT Facility.

(3) Experiments should be performed in the RENT Facil-
    ity to establish the requirements to be placed
    on an operating LDV system.

(4) Additional laboratory experiments on surface
    roughness techniques be conducted, leading to
    preliminary experiments in the RENT Facility
    itself.

REFERENCES

1. Anonymous, "The 50 Megawatt Facility of the Air
    Force Flight Dynamics Laboratory Information for
    Users," Third Edition, AFFDL TM 75-39-FXE,
    September 1975.

2. Carpenter, R. F., "A Laser Shadowgraph for Flow
    Visualization in the AFFDL RENT Facility,"
    AFFDL TM-75-46-FXN, June 1975.

3. Trolinger, J. D., "Laser Instrumentation for Flow
    Diagnostics," AGARDograph 186.

APPENDIX A

SHADOWGRAPH SYSTEM DESIGN EQUATIONS

The shadowgraph optical system design has considered the following criteria:

(1) A narrow pass band line filter must be used to block ambient light. Such filters operate at a limited F-number. The manufacturer's specifications for a 30 angstrom filter state that the filter should be used at F/15 or larger.

(2) The shadowgraph image must pass through a fast acting shutter, preferably one inch in diameter.

(3) The field of view should cover approximately five inches in diameter.

(4) It is preferable because of existing equipment to use a 35 mm (1.38 inch) format for the recording.

The design equations used to meet all of these conditions are shown in Figure A-1.

S — Object Distance

S^1 — Image Distance

m — Magnification

Subnumbers Designate Lens Number

Desired 5 in.

Object Plane

lens 1

$S_1 = (1 + \frac{1}{m_1})f_1$

$S_1^1 = (1+m_1)f_1$

Line Filter

Shutter

$S_2 = (1 + \frac{1}{m_1})f_2$

lens 2

ℓ_2

$S_2^1 = (1+m_2)f_2$

Desired 35mm = 1.38 in.

Example -- Object one size ~ 5 in.

Image one size ~ .9 in. $\longrightarrow$ $m_1 = \frac{.9}{5} = .18$

Object two size ~ .9 in.

Image two size ~ 1.38 in. $\longrightarrow$ $m_2 = 1.53$

If $S_1 = 84$ in. then $S_1^1 = 15.12$ in.

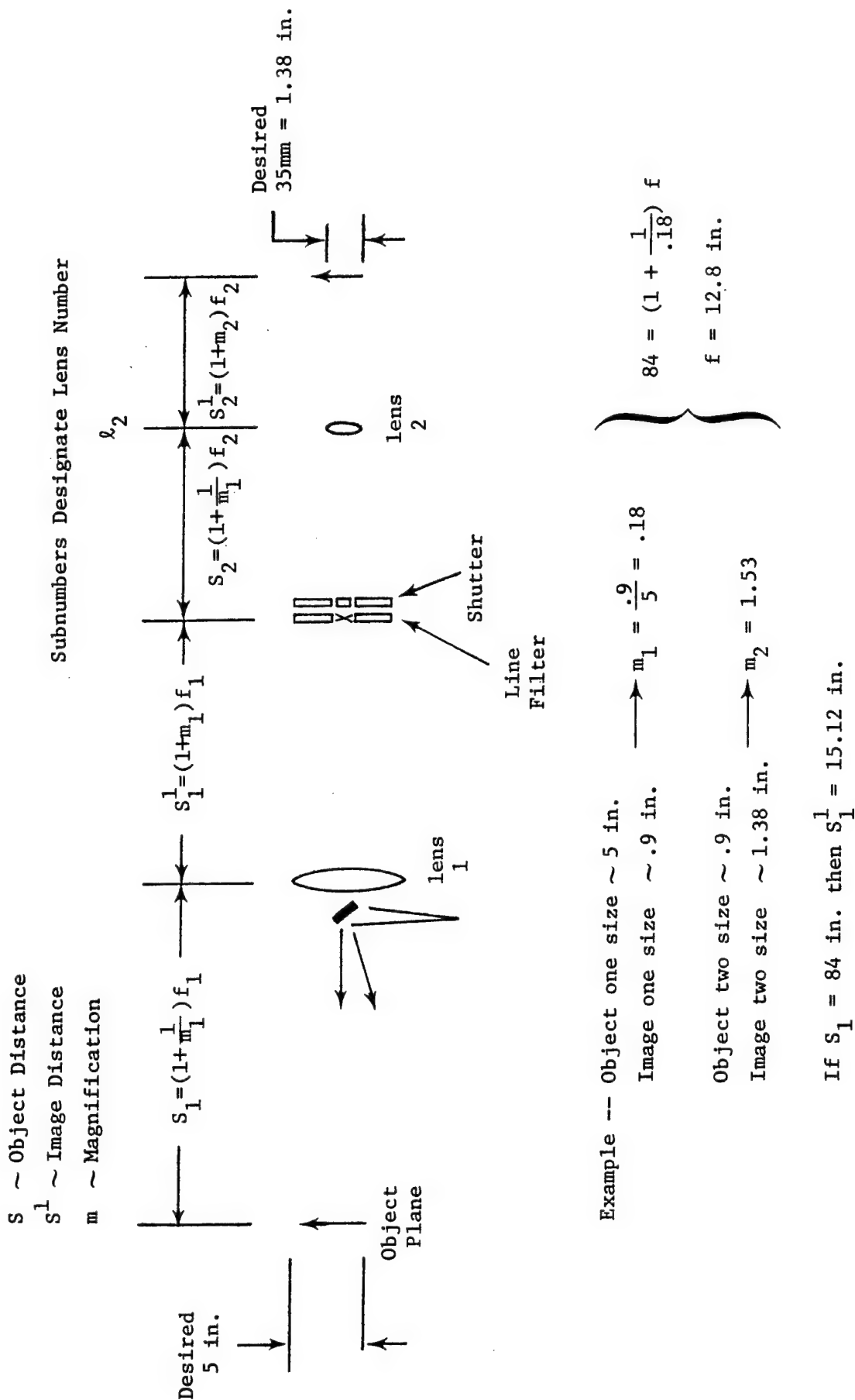$$84 = (1 + \frac{1}{.18})\,f$$

$$f = 12.8 \text{ in.}$$

Figure A-1.   Design Equations for the Shadowgraph Optics

APPENDIX B

WIRING DIAGRAMS FOR THE

RUBY LASER SHADOWGRAPH SYSTEM

NOTES FOR FIGURE 1

(1) Connector J1 (the 115 VAC power input) can be any convenient 3-pin connection, or the power cord which plugs into the wall can just be brought in through a gromet and this connector may be deleted.

(2) Switches S_1 and S_2 shall be single-pole, single-throw, normally open push-button switches and capable of handling 115 VAC @ 1 amp.

(3) Fuses F_1 and F_2 can be put in any convenient fuse-holder that will accommodate standard 3AG-size fuzes. The fuses should be capable of handling 115 VAC @ 1 amp, and be of the slow blow variety.

(4) Connectors J2 and J3 can be any convenient 3-pin connector capable of handling 115 VAC @ 1 amp.

(5) Connector J4 can be any convenient 6-pin connector which is readily available. It need only be able to handle 20 volts @ 20 Ma. The mate of this connector will be used as part of the wiring harness delineated as part of Figure 2.

(6) Lamps L_1 and L_2 need to be any convenient 12-volt incandescent bulb. They will need to be mounted in a mechanical holder. The color is not of great importance, but if you have a choice, make L_1 red and L_2 white.

(7) S_3 and S_4 shall be single-pole, single-throw, normally open push-button switches and capable of handling 20 VDC at 20 Ma.

(8) The point 0022 µf. capacitor should be any available capacitor that will stand 1 Kv. and should be mounted directly across the connection terminals of switch S_4. This capacitor must be non-polarized.
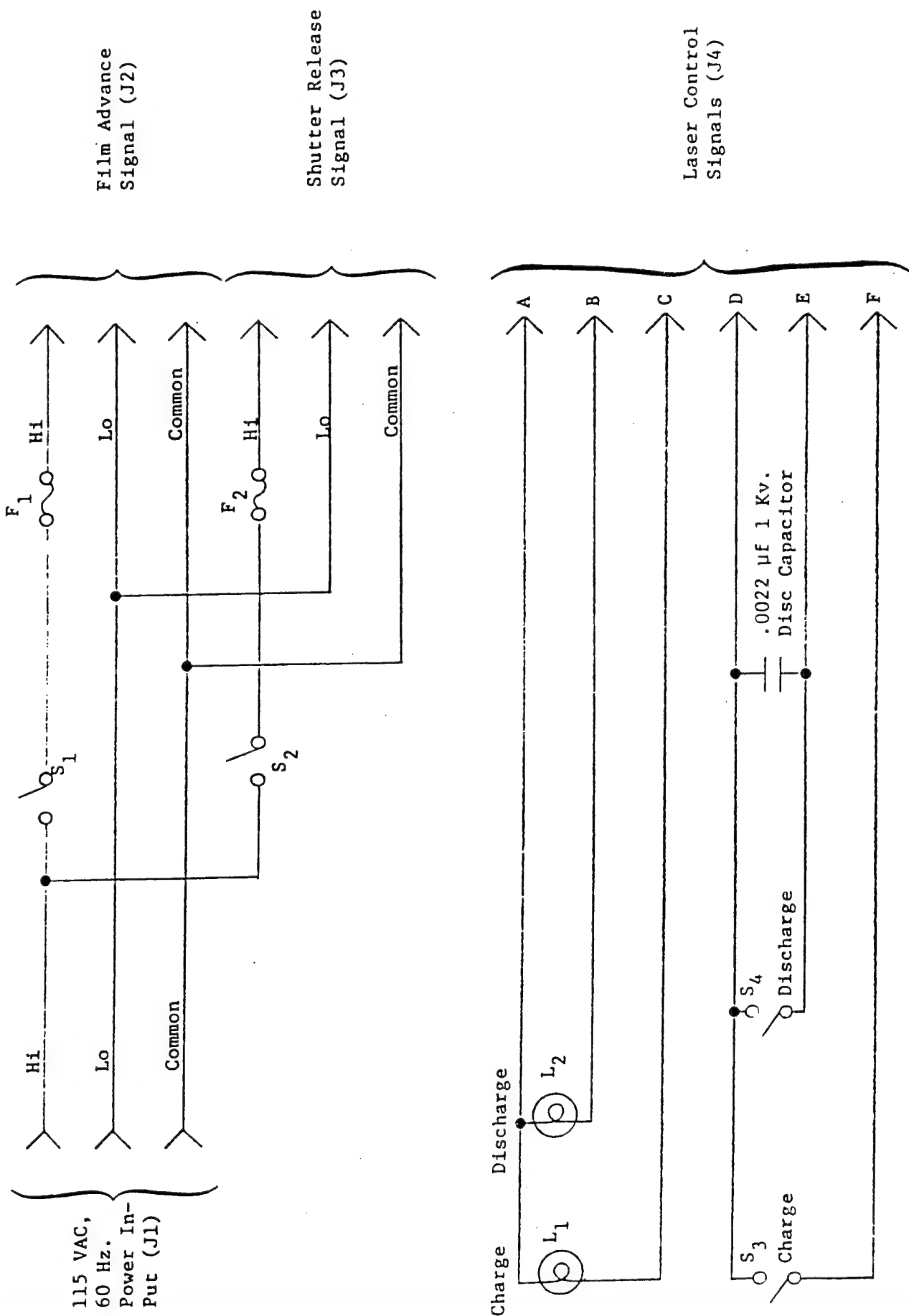
Figure B-1. Schematic for Control Panel (Mounted in Control Room)

NOTES FOR FIGURE 2

(1) Connector J4 shall be the mating connector to the one selected for J4 on the control panel.

(2) The cable from connector J4 to connector P6 on the Apollo laser should be a 6-conductor shielded cable. If this type of cable is not available, a 2-conductor shielded cable may be used for the connections from J4 pins E and F to P6 pins E and A with the shield connected to P6 pins D and K, and the other 4 wires may be regular cable with no shielding. This un-shielded condition is not the preferred case, try and use a shielded cable if at all possible.

(3) The cable from P6 pin B to the shutter sync. output shall be any standard size coaxial cable, i.e., RG 174 or RG 58. The connector to go on the shutter end of this cable will have to be chosen after the shutter is available and the type of con-nector needed can be determined.

(4) Connectors J2 and J3 for the film advance and shutter release cables are to mate with connectors J2 and J3 on the con-trol panel.

(5) Connector requirements for J5 and J6 can be determined and installed after the shutter and film transport are available for inspection.
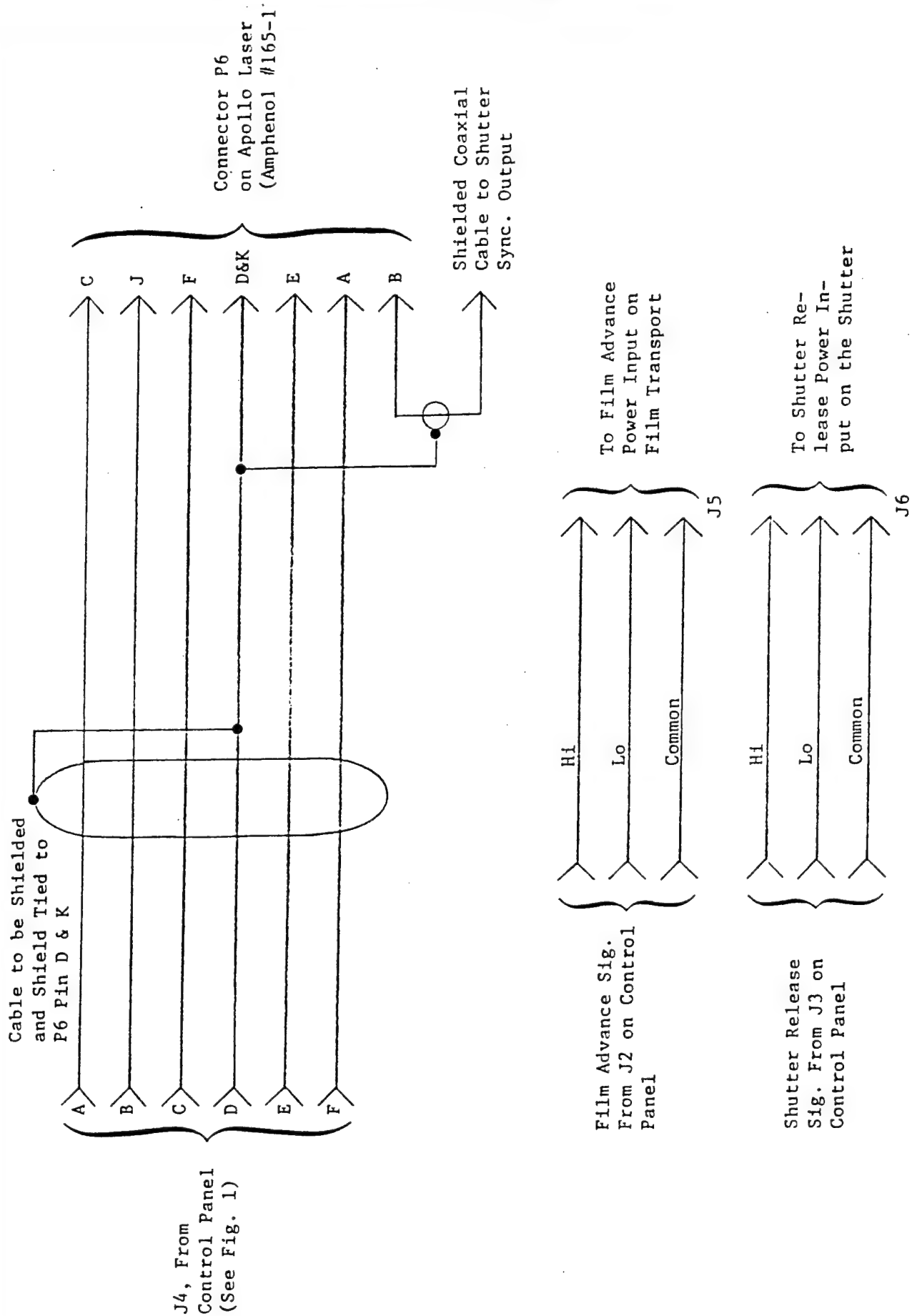
Figure B-2. Facility Cable Installation, Including Laser Control Connector and Camera-Shutter Connectors

APPENDIX C

NON-IMAGING OPTICAL METHODS

(Adapted from an unpublished report by K. D. Jones)

The following section describes the principles of operation of some non-imaging optical methods developed for surface roughness characterization. Most industrial surface roughness applications occur on engineering materials of sufficient thickness to make them opaque. This limits the characterization of these surfaces to non-transmittive phenomena. Reflection is the most intensively studied light interaction and has been applied to the majority of studies concerning the non-imaging methods of gloss and scatter. Diffraction effects are also evident, primarily in scattering techniques and shallow angle reflection methods.

Gloss Measurement

The earliest method of evaluating a rough surface was by observing the amount of light reflected by the surface or its gloss. If the surface was relatively smooth, it would reflect more light than a rougher surface. Advancements in industrial technology eventually demanded a more scientific approach to gloss.

The first objective was to define gloss in terms of its physical properties. Lichthardt[1] found 44 definitions of gloss in published literature. Gloss has been determined to be independent of color but is dependent on the surface's ability to function as a mirror and to reflect light in different directions[2].

Reflected light intensity can be plotted on polar or rectangular coordinates in two or three dimensions. The plane of incidence is perpendicular to the surface lay (the direction of

the predominant surface roughness characteristic) to provide as great a distribution as possible.

Theoretical treatment of the relation between gloss and surface roughness has been carried out from different viewpoints with different results. Bennett[3] uses diffraction theory, provided the surface irregularities are small compared to the wavelength of incident light. He states the r.m.s. value of the surface may be accurately found using infrared light; however, only for values less than 0.25 μm (10 uin). Motyčka[4] describes gloss in terms of phase changes at the surface due to reflection. The reflected light intensity (R_{os}) from a real surface then becomes less than the intensity of reflected light for an ideal surface (R_o) and the ratio R_o/R_{os} may be related to r.m.s. roughness. Schlötterer[5] defines a ground surface as a number of parallel grooves of equal width and depth. By combining Huygens' principle and light superposition theory at all angles, he shows the intensity curve is a singular function of the groove parameters. He concludes that the highest reflection intensity values are received when irregularities are small compared to the wavelength in agreement with Bennett.

Both Bennett and Motyčka use the r.m.s. value because it is a statistical property which represents the standard deviation about a mean line. According to Motyčka, the R_a (CLA) value depends on both the distribution and slope of the irregularities; therefore, the R_a value is not a singular function of a surface parameter. Even so, testing on ground and polished surfaces has shown that R_a and r.m.s. values follow each other very well though the r.m.s. values tend to be approximately 11 percent higher.

All three of the theories presented describe the reflection ability or gloss of a surface as a singular function of its geometry. Bennett claims that his results can be used on all surfaces,

while Schlötterer's and Motycka's are mainly for ground or polished surfaces.

Instrumentation used to measure or record gloss intensity distributions are called glossmeters or goniophotometers. Glossmeters integrate the intensity signal and display it as a meter reading. The basic glossmeter[6,7] is comprised of an illuminator and a photocell. Lenses are used to collimate the illuminating light and to focus the collected reflections at the photocell (see Figure 1). Both elements are generally placed at a 45 degree angle with the surface, normal to one another. Glossmeters are divided into three major groups:

(a) Glossmeters measuring only the direct reflected light;
(b) Glossmeters measuring only the diffuse reflected light; and
(c) Glossmeters measuring both the direct and diffuse reflected light.

The intended range of glossmeter operation is 0.05-0.5 μm (2-20 uin).

Goniophotometers record the intensity distribution with respect to position (See Figure 2). Several definitions of gloss are shown in Figure 3, based on goniophotometer plots.

Scatter Theory

In addition to the large group of instruments based on gloss, the other major grouping is scatter. Modeling and testing within the scope of this term includes reflection and diffraction phenomena. A literature survey and testing by Smith and Hering[8] describes the background and status of scatter models. The basis for much of the current investigation into scatter is specular reflectance and spectral bidirectional reflectance.

Spectral bidirectional reflectance describes the spatial distribution of reflected energy due to irradiation from a prescribed direction by radiant energy within a small wavelength interval about a selected wavelength (monochromatic light). For brevity,
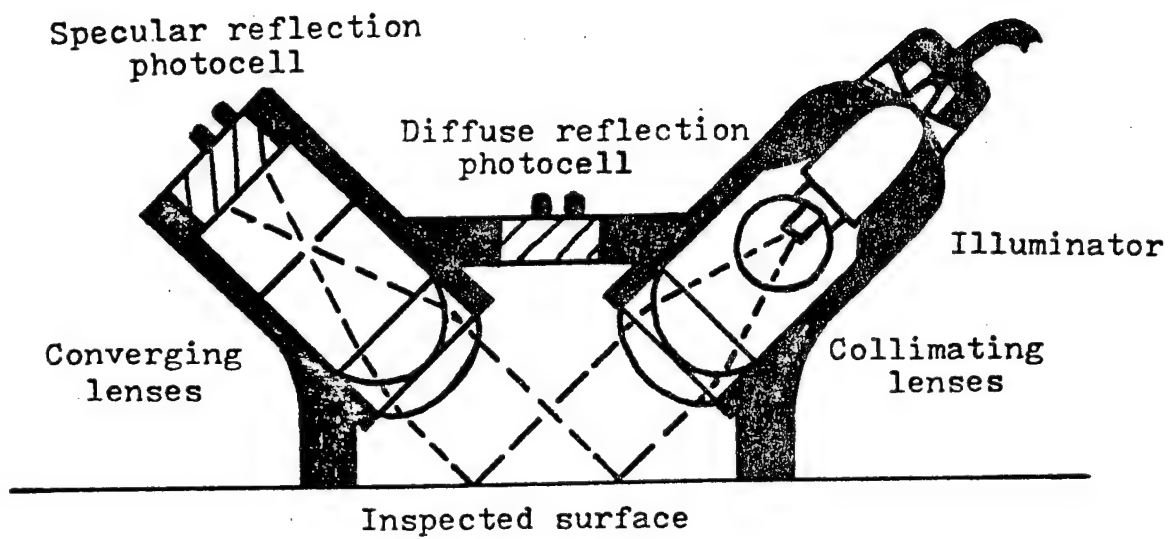
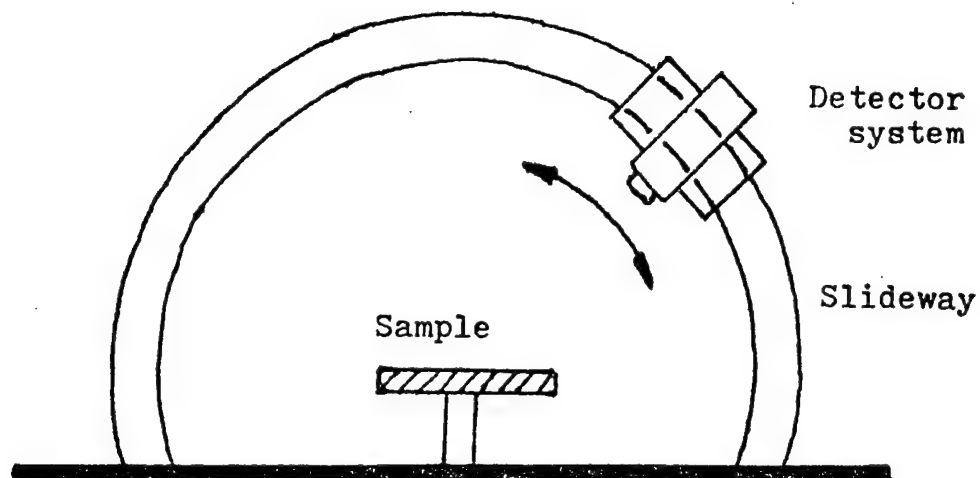Figure C-1. Schematic of a Simple Glossmeter

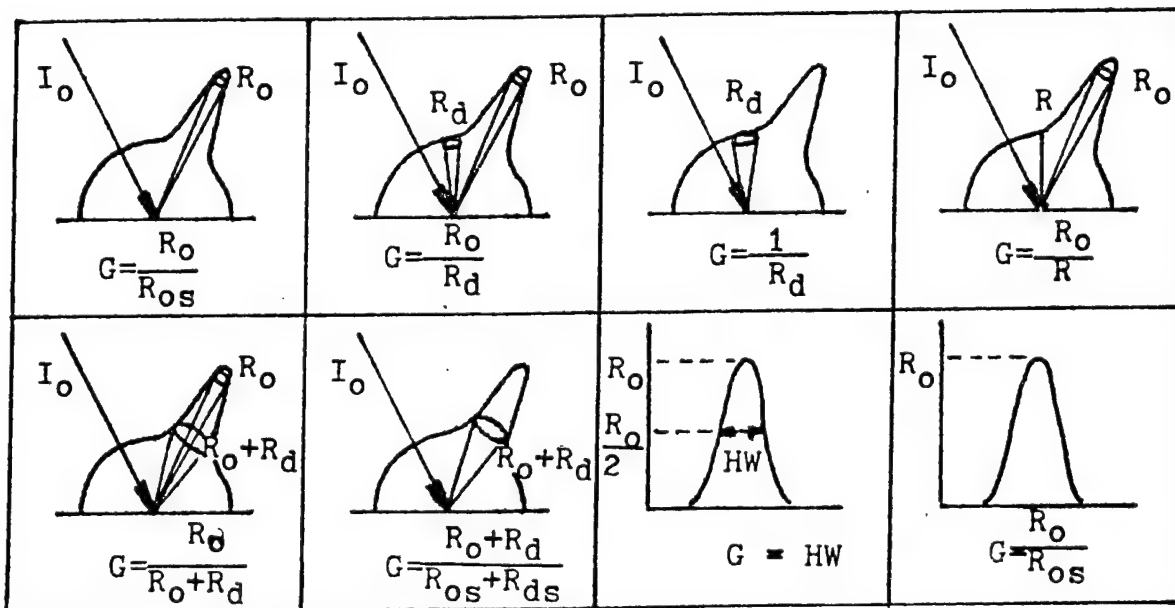Figure C-2.   Schematic of a Simple Goniophotometer

Figure C-3.   Definitions of Gloss

bidirectional reflectance is denoted by BDR and, unless otherwise stated, all radiative properties are understood to be monochromatic. Experiments[9-19] confirm that BDR is strongly dependent upon direction and wavelength of incident energy as well as the surface characteristics. Directions of incidence and reflection contained within hemispherical space above a considered surface are the factors of interest. The wavelength range of importance is 0.2-100 μm since the major contribution of radiant energy as a result of visible irradiation and that emitted by engineering materials is found in this wavelength range. Specification of chemical, physical, and topographical characteristics is necessary to describe a surface. Emphasis is given here to the influence of surface roughness on BDR for materials sufficiently thick to be considered opaque. Surface roughness is commonly expressed in terms of root mean square (r.m.s.) height[20*] measured from a mean surface plane. Typical r.m.s. heights for surfaces produced by common engineering production methods are within the range 0.01-10 μm (0.4-400 uin)[20]. Upon examination of a rough surface profile, it is realized that at least one other parameter is necessary to adequately describe the surface contour. An important second parameter is r.m.s. slope, and it has received considerably less attention than r.m.s. height. Based on reported r.m.s. slopes for engineering materials surfaces, the r.m.s. slope range of interest is estimated to be 0.01-1.0[21].

A general discussion of surface roughness effects on BDR has been given by Bennett[22]. Surface roughness effects are generally categorized in terms of optical roughness. Optical roughness is

---

* Please note that r.m.s. roughness was replaced as a roughness standard by arithmetic average (AA) in 1955. However, as a statistical parameter, r.m.s. values are still used by a large number of researchers in surface texture measurement.

is defined as the ratio of a characteristic roughness height of the surface to a characteristic wavelength of incident energy. If the characteristic height is taken as the r.m.s height and the characteristic wavelength is the wavelength of incident energy, then for the previously cited ranges for these quantities, the optical roughness range of interest is approximately 0.0001-50. Unless otherwise stated, reference to surfaces of small and large optical roughness values refer to surfaces with optical roughness values less than and greater than unity, respectively.

Surface roughness effects on BDR are reviewed in relation to an optically smooth surface, a small optical roughness and a large optical roughness. In each section, BDR measurements and models are reviewed. A summary of the basic findings is presented at the end of the chapter.

o   Optically Smooth Surfaces

An optically smooth surface reflects incident energy according to the laws of specular reflection which implies that reflected energy lies in the plane of incidence with identical polar angles of incidence and reflection and with equal solid angles of transfer[23]. Two general classifications of materials are considered; namely, electrical conductors and nonconductors. Measurements[24] confirm that specular reflectance, denoted by SPR, for both materials is nearly independent of direction less than 50 degrees. Furthermore, nonconductors have a relatively small value for SPR at normal incidence that increases with increasing polar angle of incidence. Conductors have a large value for SPR at normal incidence that decreases slightly with increasing polar angle of incidence until grazing incidence is attained.

SPR for an optically smooth, chemically and physically uncontaminated surface can be predicted from solution of the Maxwell equations of electrodynamics. The solution is expressed in terms of the Fresnel equations[25,26]. SPR for unpolarized incident energy is given in terms of polar angle of incidence as well as wavelength dependent material properties called optical constants.

Various techniques[27-29] have been employed to evaluate the optical constants from SPR measurements. However, surface damage resulting from surface preparation may cause the optical constants of thin surface layers which are important for radiative properties of materials to differ significantly from those of the bulk material. SPR measurements[22,30] for an electropolished surface are observed to be higher than those for a mechanically polished surface. Surface damage effects, however, are not as important for wavelengths in the infrared.

o   Small Optical Roughness

It is convenient to examine surface roughness effects for small optical roughness by investigating their influence on SPR. SPR[12,13,16,31-35] for small optical roughness exhibits the following characteristics. First, SPR decreases with increasing optical roughness for fixed polar angle of incidence. Thus, as the surface becomes rougher or as the wavelength becomes shorter, the energy observed in the specular direction decreases. This could be a result of increased scattering by, or multiple reflections within, surface roughness elements. For fixed optical roughness, SPR increases with increasing polar angle of incidence. Thus, the surface becomes more specular as polar angle of incidence increases.

BDR measurements[12-14,16,34-36] for small optical roughness exhibit the following characteristics. For optical roughness values less than 0.05, BDR distributions are similar to those for specular reflection. As optical roughness exceeds this value, greater amounts of reflected energy are observed in directions of reflection other than near the specular direction. For fixed optical roughness, BDR distributions approach those for specular reflection as polar angle of incidence approaches grazing incidence. Furthermore, BDR distributions attain maxima in the specular direction for optical roughness values less than approximately

$0.5^{(14)}$. For larger optical values, however, the maxima occur at polar angles of reflection greater than the specular direction.

Theoretical investigations that attempt to describe surface roughness effects on BDR for small optical roughness are based on diffraction effects. Numerous diffraction models have been developed in connection with reflection of radio and radar waves from rough surfaces. A review of these models and relevant literature is available in a book by Beckman and Spizzichino[37]. Although more recent BDR models have been suggested[38,39], a complete examination of these models in view of engineering application and BDR measurements is lacking. The Beckman model has been previously examined by Houchens and Hering[40] and Smith and Hering[41] and shown to have a wider range of engineering application than some other models. Beckman developed his model for a perfectly conducting rough surface. Since absorption is absent, the model essentially describes surface roughness effects on the spatial distribution of reflected energy. The rough surface was taken isotropic with a statistical description for the roughness elements. Comparisons [34,36,40] of the Beckman model with SPR and BDR measurements demonstrate that the model exhibits similar characteristics as the measurements for optical roughness values less than 0.2 and for near-normal incidence. As previously noted[34,40], there are insufficient measurements available for well documented rough surfaces to substantiate conclusively BDR models for small optical roughness values.

o   Large Optical Roughness

Characteristics of SPR measurements for large optical roughness are not as well defined as those for small optical roughness. Toporets[42] reported SPR measurements for polar angles of incidence less than 80 degrees that exhibit the following characteristics. SPR increases with increasing optical roughness

for fixed polar angle of incidence. Moreover, for fixed optical roughness, SPR decreases with increasing polar angle of incidence. These characteristics are contrary to those observed for small optical roughness. SPR measurements[43-45] for polar angles of incidence greater than 80 degrees exhibit similar characteristics as those for small optical roughness. BDR measurements[13-16,35,46-48] for large optical roughness exhibit the following characteristics. As optical roughness increases, greater amounts of reflected energy are found in directions of reflection further removed from the specular direction. The diffuse reflection limit[23] in which the intensity of reflected energy is uniform over hemispherical space is attained only for near-normal incidence[13-15,18,19]. For other than near-normal incidence, BDR distributions exhibit maxima in the plane of incidence at polar angles of reflection greater than the specular direction. As optical roughness increases, these so-called off-specular peaks occur at polar angles of reflection further removed from the specular direction. As polar angle of incidence approaches grazing incidence, BDR distributions are similar to those for specular reflection. BDR measurements reported by Voishvillo[49] for polar angle of incidence of 70 degrees exhibit a peak in the specular direction as well as a smaller peak at polar angles of reflection greater than the specular direction.

Theoretical attempts to develop BDR models that describe the measurements for large optical roughness are formulated using the methods of geometrical optics. As noted by Toporets[45], however, this method applies only for directions of incidence other than near-grazing incidence. Diffraction effects must be accounted for an analyses for near-grazing incidence. SPR measurements for polar angles of incidence greater than 80 degrees[43,45] were correlated with an expression similar to that for the specular component of the Beckman model[40]. BDR models

have been developed for surfaces composed of mirror-like roughness elements[21,48-53] as well as diffusely reflecting roughness elements[53]. The roughness element dimensions are taken to be large relative to wavelength of incident energy. Although wavelength does not appear in the expressions developed, the models are wavelength dependent since the reflectance of the roughness element surfaces is generally wavelength dependent. For surfaces composed of mirror-like roughness elements, a statistical distribution function has been utilized to specify the probability that a surface area contains roughness elements of a given slope. The roughness parameter employed in the distribution function is related to r.m.s. slope. For surfaces composed of diffusely reflecting roughness elements, the roughness element slopes have been assumed equal. Hence, BDR models for large optical roughness are independent of optical roughness. Diffraction models[40,54] for large optical roughness are also expressed only in terms of r.m.s. slope. Since a very limited amount of information is available for the r.m.s. slope of engineering materials, the importance of this surface roughness parameter for correlating BDR measurements and models has not been established. Comparison of BDR models with measurements have almost always been performed by adjusting the parameters of the models until reasonable agreement is obtained. Comparison [48,51,55] of BDR models[48,50,51] with reported BDR measurements illustrates that the models do exhibit characteristics similar to those of the measurements.

o   Summary of Surface Roughness Effects

The above discussion based on the work of Smith and Hering[8] reveals the following concerning surface roughness effects on BDR:

(a)   Experiments confirm that BDR is strongly dependent upon direction and wavelength of incident energy as well as surface topography.

(b)   At least two surface roughness parameters are necessary to characterize the surface profile; namely, r.m.s.

height and r.m.s. slope. The r.m.s. height has
received considerably more experimental investi-
gation than r.m.s slope. Both parameters, however,
have been theoretically investigated.

(c)   Surface roughness effects on BDR measurements are
conveniently discussed in terms of optical roughness.
As optical roughness approaches zero, the specular
reflection limit is reached. Diffuse reflection is
attained only for large optical roughness and for
near-normal incidence. Off-specular peaks are ob-
served for other than near-normal incidence for
large optical roughness.

(d)   BDR models have been developed by utilizing the
concepts of physical and geometrical optics and
are applicable to small and large optical roughness
values, respectively. BDR models for small optical
roughness are expressed in terms of r.m.s. height and
slope, but only r.m.s. slope appears in BDR models
for large optical roughness.

(e)   Comprehensive comparisons of analytical models with
measurements are lacking. BDR measurements are
inadequate both in quantity and scope for confirm-
ation of any BDR model.

REFERENCES

1. Lichthardt, U., Mitterlunger Forschung Gebiete, Blechverarb, No. 23/24, (1961).

2. Westberg, J., "Development of Objective Methods for Judging the Quality of Ground and Polished Surfaces in Production," Properties and Metrology of Surfaces, published by the Institution of Mechanical Engineers as the Proceedings of the Institution of Mechanical Engineers, (1967-68), page 261.

3. Bennett, H. E., Industrial Quality Control, No. 8 (February 1964), pages 18-23.

4. Motyčka, J., Bestimmung der Oberflaechenrauhigkeit durch Lichtreflexion, Technische Hochschule-Int. Kolloquim, 10th (Technische Optik) Ilmenau, n8 (1965), pages 77-81.

5. Schlötterer, H., Metalloberfläche, No. 2 (February 1962), pages 49-52; No. 3 (March 1962), pages 81-4; No. 5 (May 1962), pages 141-7.

6. American Society for Testing and Materials, "Recommended Practice for Goniophotometry of Reflecting Optics and Materials," ASTM Designation E 167-63, (1970), available from ASTM, 1916 Race St., Philadelphia, Pa. 19103.

7. American Society for Testing and Materials, "Recommended Practice for Selection of Geometric Conditions for Measurement of Reflectance and Transmittance," ASTM Designation E 179-73, (1970), available from ASTM, 1916 Race St., Philadelphia, Pa. 19103.

8. Smith, T., and Hering, R., Surface Roughness Effects on Bidirectional Reflectance, University of Illinois at Urbana, Champaign, Illinois, No. ME-TR-661-2, (June 1972), pages 3-10.

9. Eckhert, E. R. G., "Messung der Reflexion von Wärmstrahlen an Technischen Oberflachen," Forschung auf dem Gebiete des Ingenieurwessens, 7 (1936), page 265

10. Münch, B., "Die Richtungsverteilung bei der Reflexion von Wärmestrahlung und ihr Einfluss aur die Wärmeübertragung." Mitterlunger aus dem Institute fur Thermodynmak und

Verbrennungsmotoranban au der Eidgenossischen Technischen Honschule in Qurich, No. 16 (1955).

11. Agnew, J. T. and McQuistan, R. B., "Experiments Concerning Infrared Diffuse Reflectance Standards in the Range 0.8 to 20.0 Microns," Journal of the Optical Society of America, 43 (1953), page 999.

12. Birkebak, R. C. and Eckert, E. R. G., "Effects of Roughness of Metal Surfaces on Angular Distribution of Monochromatic Reflected Radiation," Transcript ASME, Journal of Heat Transfer, 87C (1965), page 283.

13. Torrance, K. E. and Sparrow, E. M., "Biangular Reflectance of an Electric Nonconductor as a Function of Wavelength and Surface Roughness," Transcript ASME, Journal of Heat Transfer, 87C (1965), page 335.

14. Torrance, K. E. and Sparrow, E. M., "Off-Specular Peaks in the Directional Distribution of Reflected Thermal Radiation," Transcript ASME, Journal of Heat Transfer, 88C (1966), page 223.

15. Herold, L.M. and Edwards, D. K., "Bidirectional Reflectance Characteristics of Rough, Sintered-Metal and Wire-Screen Surface Systems," American Institute for Astronautics and Aeronautics Journal, 4, (1966), page 1802.

16. Love, T. J. and Francis, R. E., "Experimental Determination of Reflectance Function Type 302 Stainless Steel," Progress in Astronautics and Aeronautics, Academic Press, New York, (1967).

17. Collignon, F., "Etude des Indicatrices de Reflexion d'une Surface Rugueuse Soumise au Rayonnement Thermique," Revue Generale de Thermique, 8 (1969), page 733.

18. Shcherbina, D. M., Kirichenko, A. P., and Aliev, R. S., "Characteristic Reflection Curves with Normal Irradiation of a Surface," High Temperature, 6 (1968), page 351.

19. Shcherbina, D.M. and Kirichenko, A.P., "Precision in Measuring the Emissivity Factor in Reflecting Furnaces," Measurement Technology, 7 (1968), page 871.

20. American Standards Association, "Surface Texture," ASA Standard B46.1, (1962).

21. Smith, T. F. and Hering, R. G., Bidirectional Reflectance of a Randomly Rough Surface, American Institute for Astronautics and Aeronautics Paper No. 71-46 from the Sixth Thermophysics Conference, (April 1971).

22. Bennett, H. E., Influence of Surface Roughness, Surface Damage and Oxide Films on Emittance, from the Symposium on Thermal Radiation of Solids, National Aeronautics and Space Administration Paper No. SP-55 (1965), page 145.

23. Sparrow, E. M. and Cess, R. D., Radiation Heat Transfer, Brooks-Cole, Belmont, Ca. (1966).

24. Brandenberg, W. M., "The Reflectivity of Solids at Grazing Angles," Measurement of Thermal Radiation Properties of Solids", National Aeronautics and Space Administration Paper No. SP-31 (1963), page 75.

25. Holl, H. B., "Specular Reflection and Characteristics of Reflected Light," Jourhal of the Optical Society of America, 57 (1967), page 683.

26. Hering, R. G. and Smith, T. F., "Surface Radiation Properties from Electromagnetic Theory," International Journal of Heat and Mass Transfer, 11 (1968), page 1567.

27. Ruiz-Urbieta, Sparrow, E. M. and Eckert, E. R. G., "Methods for Determining Film Thickness and Optical Constants of Films and Substrates," Journal of the Optical Society of America, 61 (1971), page 351.

28. Beattie, J. R. and Conn, G.K.T., "Optical Constants of Metals in the Infrared--Principles of Measurement," Philadelphia Magazine, 46 (1955), page 222.

29. Juenker, D. W., "Digital Evaluation of the Complex Index of Refraction from Reflectance Data," Journal of the Optical Society of America, 55 (1965), page 295.

30. Jones, M. C. and Palmer, D. C., "A Technique for the Measurement of Spectral Reflectance at Low Temperatures in the Infrared and Far Infrared," Progress in Astronautics and Aeronautics, 21 (1969), page 543.

31. Gorton, A. F., "Reflection from, and Transmission through, Rough Surface," _Physics Review_, 7 (1916), page 66.

32. Bennett, H. E., "Specular Reflectance of Aluminized Ground Glass and the Height Distribution of Surface Irregularities," Journal of the Optical Society of America, 53 (1963), page 1389.

33. Bennett, H. E. and Porteus, J. O., "Relation Between Surface Roughness and Specular Reflectance at Normal Incidence," Journal of the Optical Society of America, 51 (1961), page 123.

34. Smith, T. F. and Hering, R. G., _Comparison of Bidirectional Reflectance Measurements and Model for Metallic Surfaces_, from the American Society of Mechanical Engineers Proceedings of the Fifth Symposium on Thermophysical Properties, (1970), page 429.

35. Povey, M. and Fabre, D., "Quelques Experiences de Diffusion du Rayonnement Ultraviolet par des Surfaces Rugueuses," _Optica Acta_, 16 (1969), page 471.

36. Latta, M. R., "The Scattering of 10.6 Micron Radiation from Ground Glass Surfaces," _Journal of the Optical Society of America_, 59 (1969), page 493.

37. Beckmann, P. and Spizzichino, A., _The Scattering of Electromagnetic Waves from Rough Surfaces_, The MacMillan Co., New York (1963).

38. Leader, J. D., "Multiple Scattering of Electromagnetic Waves from Rough Surfaces," Jourhal of the Optical Society of America, 60 (1970), page 1552.

39. Hunderi, O. and Beaglehole, D., "Study of the Interaction of Light with Rough Metal Surfaces. II. Theory.," _Physics Review_, B.2 (1970), page 321.

40. Houchens, A. F. and Hering, R. G., "Bidirectional Reflectance of Rough Metal Surfaces," _Progress in Astronautics and Aeronautics_, 20 (1967), page 65.

41. Smith, T.F. and Hering, R. G., _Comparison of the Beckmann Model with Bidirectional Reflectance Measurements_, from the American Society of Mechanical Engineers - American Institute for Chemical Engineers Heat Transfer Conference, Atlanta (1973).

42. Toporets, A. S., "Specular Reflection of Light from a Rough Surface," _Optical Spectry_, 24 (1968), page 62.

43. Gordinskii, G. M., "The Statistical Interference of Light upon Reflection from Matte-Gloss Surfaces," _Optical Spectry_, 15 (1963), page 57.

44. Middleton, W. E. K. and Wyszecki, G., "Colors Produced by Reflection at Grazing Incidence from Rough Surfaces," _Journal of the Optical Society of America_, 41 (1957), page 1020.

45. Toporets, A. S., "Specular Reflection from a Rough Surface," _Optical Spectry_, 16 (1964), page 54.

46. Povey, M., Fabre, D., and Romand, J., "Indicatrices de Diffusion dans l'ultraviolet Lointain," _Optica Acta_, 15 (1968), page 159.

47. Vanetsian, R. A., Lebedeva, L. P., Krayushkina, V. A. and Ivanovskaya, A. S., "Diffusion Reflection of Laser Radiation," _Soviet Journal of Optical Technology_, 36 (1969), page 251.

48. Leader, J. C., Bidirectional Scattering of Electromagnetic Waves from Rough Surfaces, a report for McDonnell-Douglas, No. MDC-70-022, (1970).

49. Voishvillo, N. A., "Reflection of Light by a Rough Glass Surface at Large Angles of Incidence of the Illuminating Beam," _Optical Spectry_, 22 (1967), page 517.

50. Torrance, K. E. and Sparrow, E. M., "Theory for Off-Specular Reflection from Roughened Surfaces," _Journal of the Optical Society of America_, 57 (1967), page 1105.

51. Look, D. D., Jr. and Love, T. J., Investigation of the Effects of Surface Roughness upon Reflectance," _Progress in Astronautics and Aeronautics_, 24 (1970), page 123.

52. Smith, A. M., Müller, P. R., Frost, W., and Hsia, H., "Super and Sub-Specular Maxima in the Angular Distribution of Polarized Radiation Reflected from Roughened, Dielectric Surfaces," _Progress in Astronautics and Aeronautics_, 24 (1970), page 249.

53. Hering, R. G. and Smith, T. F., "Apparent Radiation Properties of a Rough Surface," _Progress in Astronautics and Aeronautics_, 23 (1970), page 337.

54. Povey, M., "Vacuum Ultraviolet Reflective Scattering Distributions," Optica Acta, 1 (1969), page 105.

55. Treat, C. H. and Wildin, M. W., "Investigation of a Model for Bidirectional Reflectance of Rough Surfaces," Progress in Astronautics and Aeronautics, 23 (1970), page 77.